universität wien

DIPLOMARBEIT

Titel der Diplomarbeit

„ Towards the Functional Characterisation of Inner Brain Opsins in Medaka and Zebrafish “

Verfasserin

Susanne Bloch

angestrebter akademischer Grad

Magistra der Naturwissenschaften (Mag.rer.nat.)

Wien, 2011

Studienkennzahl lt. Studienblatt:	A 490
Studienrichtung lt. Studienblatt:	Diplomstudium Molekulare Biologie
Betreuerin:	Dr. Kristin Tessmar-Raible

Acknoledgement

There are many people to thank! First of all I would like to thank my supervisor Kristin Tessmar-Raible for her support and patience during my project and for her never-ending enthusiasm and encouragement. I want to thank her as well as Florian Raible for always having an open ear and door for questions and discussions. Futhermore many thanks to everybody of the Tessmar and Raible groups for creating such a great work environment, especially Ruth Fischer for her help with my project and and Claudia Lohs for her patience with my many questions. Finally I would like to thank my family for always supporting me.

Table of Contents

List of figures

List of symbols

AHT	Anhydrotetracycline
BAC	Bacterial Artificial Chromosome
CMLC2	Cardiac Myosin Light Chain2
CNS	Central Nervous System
c-Opsin	Ciliary opsin
CSF	Cerebrospinal Fluid
CVO	Circumventricular Organ
DIG	Digoxigenin
Dr	*Danio rerio*
DSB	Double Strand Break
DTT	Dithiothreitol
E2N	EGFP-F2A-NTR
EGFP	Enhanced Green Fluorescent Protein
F2A	Ribosomal skip site
FACS	Fluorescence Activated Cell Sorting
FRT	Flip Recombinase Target Site
GPCR	G-Protein coupled receptor
HRM	High Resolution Melting Curve
ipRGC	Intrinsically photoreceptive retinal ganglion cell
MTO	Multiple Tissue Opsin
NHEJ	Non-homologous end joining
NTR	Nitroreductase
OC	Optic chiasm
Ol	*Oryzias latipes*
PFA	Paraformaldehyde
PTU	Phenylthiourea
PTW	Phospate-buffered saline with 0,1% Tween-20
RGR-opsin	RPE retinal G protein-coupled receptor
RPE	Retinal Pigmented epithelium
RT-PCR	Reverse Transcriptase PCR
SCN	Suprachiasmatic Nucleus

TMD	Transmembrane Domain
TMT	Teleost Multiple Tissue
TRITC	Tetramethylrhodamine-5-(and 6)-isothiocyanate
VA/VAL-Opsin	Vertebrate Ancient/ Vertebrate Ancient Long Opsin
ZFD	Zinc Finger Domain
ZFN	Zinc Finger Nuclease
ZFP	Zinc Finger Protein

1 Introduction

1.1 Non-visual photoreception in vertebrates

Photoperiodicity has long been recognized as an important stimulus for the synchronization of many physiological and behavioural changes for most organisms on the planet. Circadian, circannual or seasonal rythms depend on the primary *zeitgeber* light (1) and biological clocks have to be provided with photic information in order to regulate responses to varying conditions (2). Therefore animals employ non-visual photoreceptors that provide this information.

In vertebrates photoreceptors are present in a variety of body regions, distinctly in tissues derived from the diencephalic forebrain. These can be classified as an intracranial pineal organ (*epiphysis cerebri*), an intracranial parapineal organ in bony fish and lampreys, an extracranial 'third eye' in amphibians, the lateral eyes, that also encompass the visual system, and the deep brain photoreceptors (2-4) (Figure 1.1). This abundance of cerebral photoreceptive sites suggests that the brain does not only process photic information from the periphery, but is directly involved in the sensory process.

With the discovery of photosensitive sites within the central nervous system the question of molecular players in non-image forming light detection arose. While rod and cone photoreceptors have been correlated with visual signal transduction (5), a variety of novel classes of photosensory pigments has been observed to be expressed in the deep brain. These include vertebrate ancient (VA) and vertebrate ancient long (VAL-) opsin (6), exo-rhodopsin (7) in zebrafish, pinopsin and parapinopsin in birds and lizards (8-9) or melanopsin, involved in the regulation of melatonin levels. The circadian photopigment melanopsin is present in the hypothalamus in some, and the retinal ganglion cells of the eye in all vertebrate phyla (10). In the course of my project I will focus on two other families of non-visual opsins that have been shown to be present in the vertebrate brain, i.e. the Teleost Multiple Tissue (TMT) opsins and Encephalopsin.

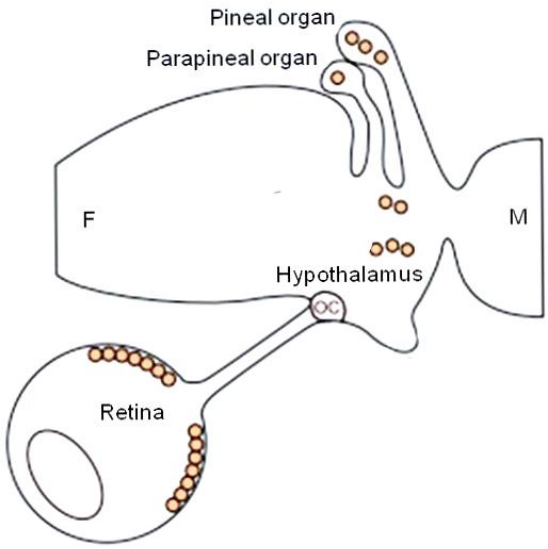

Figure 1-1: Photoreceptive sites in the teleost brain

Regions derived from the diencepahlic forebrain have been demonstrated to be photoreceptive. Here the pineal and parapineal organ and the hypothalamic structures as well as the photoreceptors within the retinal ganglion cells of the eyes are schematically depicted.
OC- optic chiasm, F- forebrain, M – midbrain (Figure adapted from (2))

1.2 The system of cerebrospinal fluid-contacting neurons and ocular photoreception

Vigh et al. described that deep brain photoreceptors are located in the hypothalamic and septal nuclei. These are part of a system of cerebrospinal fluid (CSF)- contacting neurons (11). CSF-contacting neurons are found in the so called circumventricular organs (CVOs), such as the pineal gland or paraventricular organ among others (12). In these regions the blood-brain barrier is permeable. This means that here transduction of information between *liquor cerebrospinalis*, the fluid that fills the cavities inside and around the brain, neurons and blood can occur. CVOs contain both sensory and secretory neurons and have been ascribed a role in the control of physiological functions such as regulation of growth, blood pressure, sleep, reproduction and biological rythms (12).The pineal organ is among the oldest CVOs that have been identified in almost all vertebrate phyla and CSF-contacting neurons can be regarded as an ancient cell type located on the external surface of the brain where they send a ciliated dendritic process from the brain ventricles into the CSF.

They have been demonstrated in the hypothalamic nuclei as well as in the region of the spinal chord (13).

Also the bipolar neurons of the inner retina can be regarded as CSF-contacting neurons due to their cytological characteristics (11, 13). Among them melanopsin-expressing retinal ganglion cells that project into the suprachiasmatic nucleus (SCN), the central pacemaker of the mammalian circadian system, can be classified as intrinsically photoreceptive retinal ganglion cells (14). In fish VA opsin and its isoforms were identified in a subset of horizontal and amacrine cells in the inner retina (6, 15). This shows that, besides the rod and cone photoreceptors of the visual pathway, a system of non-visual photopigments is present in the inner nuclear layer of the vertebrate retina whose functions are still not known in detail. The anatomy of the CSF-contacting neuronal system is summarized in figure 1.2.

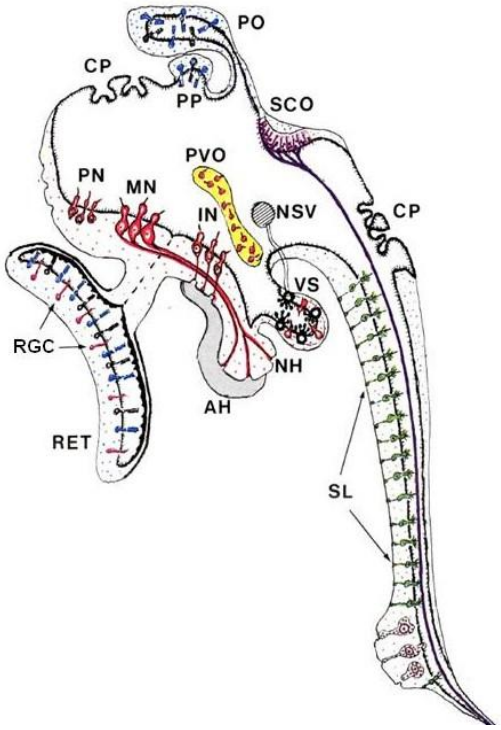

Figure 1-2: The system of cerebrospinal fluid-contacting neurons

Here there CSF-contacting neurons in the vertebrate brain are depicted. Hypothalamic neurons are highlighted in red, CSF-contacting neurons of the spinal chord are shown in green and the paraventricular organ in yellow. CSF-contacting neurons are considered the most ancient type of vertebrate nerve cells and are suggested to harbour non-visual photopigments involved in the regulation of photoperiodism (11, 16). Figure adapted from (13). AH adenohypophysis, CP choroid plexus, IN infundibular nucleus, MN magnocellular preoptic and paraventricular neurosecretory nuclei, NH neurohypophysis, NSV nucleus of the vascular sac, PN parvocellular preoptic nucleus, PO pineal organ, PP parapineal organ, PVO paraventricular organ, RET retina, RGC retinal ganglion cells, SC0 subcommissural organ, SL spinal CSF-contacting neurons, VS vascular sac.

1.3 The Opsins

1.2.1 The Opsin Families

As members of the superfamily of G-protein coupled receptors (GPCRs), the opsins belong to one of the largest and most studied families of proteins (17). GPCRs are typically seven-transmembrane proteins that can be classified into five families, namely the glutamate, rhodopsin, adhesion, frizzled/taste2, and secretin family (18). The mode of action of GPCRs is a conformational change upon stimulation by an extracellular ligand such as a peptide, ion, nucleotide or even a photon and activation of the downstream signal transduction cascade (18). The transduction pathways vary for each receptor and the opsin family can be further subdivided in accordance to the type of G-Protein they are coupled to (19) and more clearly dependent on the type of photoreceptor cell that expresses the protein (20). These are either ciliary or rhabdomeric receptor cells which differ in their morphology. While in ciliary receptors the ciliary membrane is folded to increase the cell surface and store the opsin molecules, in rhabdomeric cells only the apical surface is folded (21-22).

The vertebrate visual and non-visual opsins as well as the G_0- and G_s-coupled opsins belong to the subtype of ciliary opsins (20). Among the rhabdomeric opsins there are the G_q-coupled opsins including melanopsin and invertebrate r- opsins (22) (Figure 1.2). The third and forth subtypes of opsins are the photoisomerases and neuropsins.

1.2.1 Encephalopsins and TMT- Opsins

As the only member of the non-visual ciliary opsins Encephalopsin is conserved up to mammals. First described in 1999 by Blackshaw et al. it was shown to be expressed in the preoptic area and the paraventricular nucleus of the hypothalamus as well as in the testes of mice (23). Also in adult eyes of mice *encephalopsin* expression was detected (24). In humans however, a study showed that it is expressed also in tissues like liver, lung and kidney as well as in the retina (25-26). Furthermore six different splice isoforms exist for Encephalopsin in humans (26) and in Medaka two isoforms were discovered (27). The function of Encephalopsin is still unclear, however it has been described to be involved in asthma susceptibility (28).

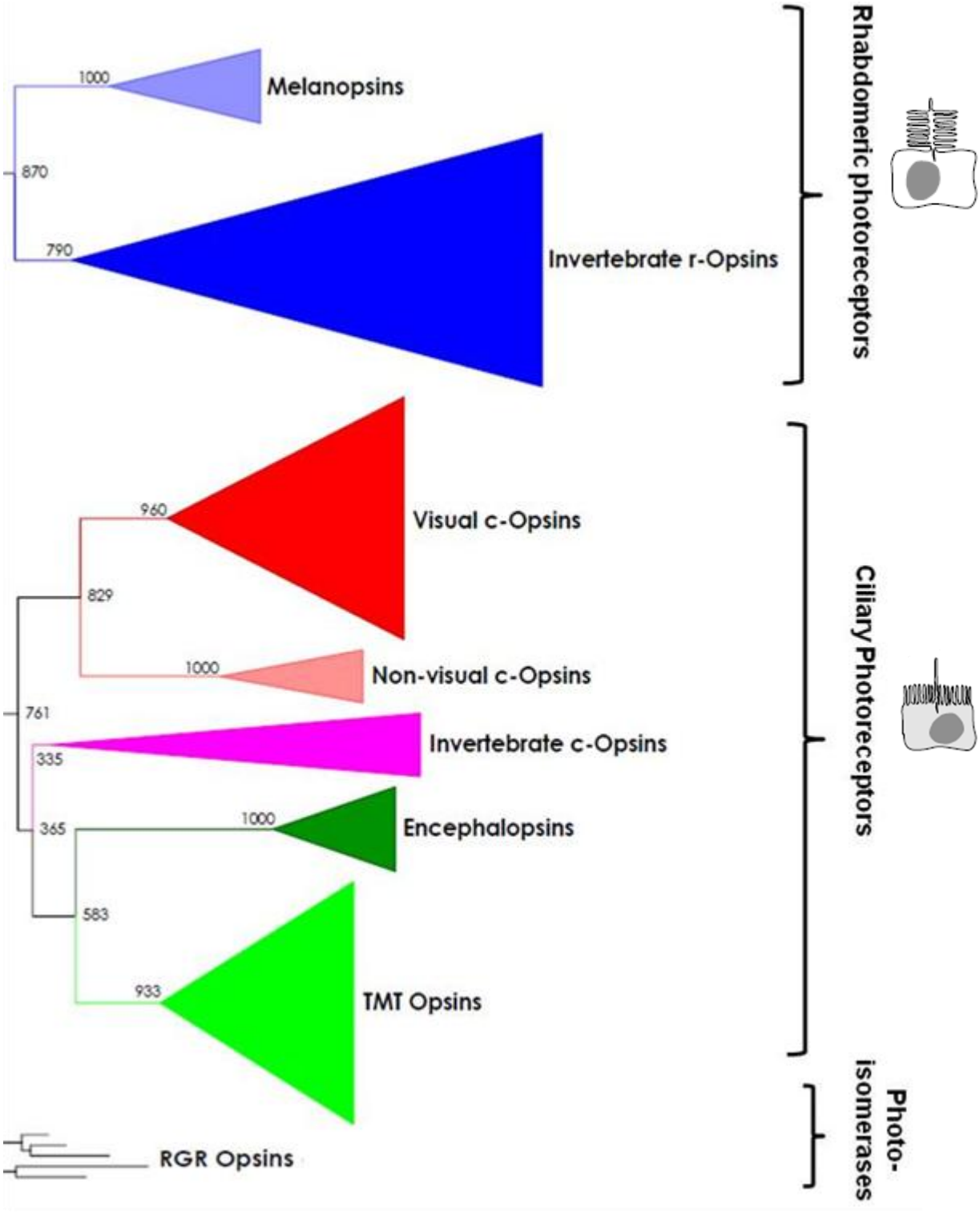

Figure 1-3: Phylogeny of the Opsin Families

Here the phylogeny of the visual and non visual vertebrate opsins in relation to other opsin families and the morphology of ciliary versus rhabdomeric photoreceptors is shown. The TMT-Opsins and Encephalopsins cluster together with the ciliary opsins, among them invertebrate r-opsins and melanopsin. The photoisomerases, here used as an outgroup, encompass the RGR-opsins, retinochrome and peropsin. (Figure adapted from (27))

In 2003 another novel family of presumptive circadian photopigments was described: the Teleost Multiple Tissue (TMT) opsins (29). Here screens of genomic libraries from Zebrafish (*Danio rerio*) and Fugu (*Fugu rubripes*) identified a member of the later termed *tmt opsin* gene family. In semi-quantitative RT-PCR analyses and cross-species RNAse Protection Assays expression in brain, liver, heart, kidney, eye and even in a PAC2 fibroblast zebrafish cell line was discovered (29). This seemingly broad expression over a variety of tissues gave the opsin family its name and lead the authors to the assumption that Multiple Tissue Opsins might be involved in the regulation of the circadian rhythm (29).

This hypothesis was strengthened in 2007 by analysis using *in situ* hybridisation methods where TMT-Opsin expression partly overlapped with that of the neuronal hormone vasotocin in discrete areas of the hypothalamus (30). Vasotocin is a member of the nonapeptide hormonal system that regulates a variety of physiological and behavioural responses, among them sexual behavior (31-32). This lead to the suggestion that TMT-Opsins play a role in photoperiod-mediated reproductive cycles. In addition to that sequence analyes and phylogenetic assays showed that the TMT-Opsins are a relatively large protein family and highly conserved in lower vertebrates (27).

There are seven opsin homologues in Zebrafish and six in Medaka (Table 1.1). These cluster together in four families: TMT-Opsin family A, B and C and Encephalopsin. TMT-Opsins and Encephalopsins are closely related, however they represent two different families among vertebrates that can be summarized as Multiple Tissue Opsins (MTOs) (27).

Opsin Family	*Danio rerio*	*Oryzias latipes*
A	Chrom. 24	Chrom. 20
	Chrom. 2	Chrom. 17
B	Chrom. 9	Chrom. 21
	Chrom. 6	
C	Chrom. 10	Chrom. 14
	Chrom. 14	Chrom. 10
Encephalopsin	Chrom. 13	Chrom. 15

Figure 1-4: Members of the TMT-Opsins and Encephalopsin in *Danio rerio* and *Oryzias latipes*

The table summarizes the TMT-Opsin and Encephalopsin homologues in Zebrafish and Medaka and the chromosome from which they are expressed. In Zebrafish there are seven homologues, in Medaka six can be found. (Data from (27))

1.4 Structural characteristics of a photoreceptor

Opsins characteristically consist of a seven-transmembrane protein coupled to the chromophore 11-*cis* retinal (Figure 1-4). The retinal is bound via a Schiff Base linkage to the lysine residue K296 (numbering according to bovine rhodopsin) in helix VII (19, 33). Binding of the retinal leads to protonation of the 11-*cis* retinal and a delocalization of the π-electrons, resulting in a shift of the absorption spectrum into the visible range (19). The protonated Schiff Base is unstable and requires a negatively charged counterion for stabilization. This amino acid is highly conserved. In most ciliary opsins a glutamate at position 113 serves as counterion while rhabdomeric opsins often employ a counterion at position 181, which can be an aspartate or glutamate (34-35). In TMT-Opsins a glutamate at position 181 acts as counterion, in Encephalopsin a negatively charged amino acid is present at postion 113 as well as at postion 181 (27). This divergence of counterion positions suggests, that most likely an ancestral opsin had the counterion at position 181, which then shifted to 113 in some vertebrate opsin families (20).

In all opsins light absorption leads to isomerisation of the retinal from the 11-*cis* to the 11-*trans* form and to a conformational change in the protein moiety (19).

This structural rearrangement of the protein exposes G-protein binding sites such as the cytoplasmatic loop between helices V and VI and a higly conserved C-terminal stretch with a characteristic sequence that distinguishes ciliary from rhabdomeric opsins (19, 27) (Figure 1-4).

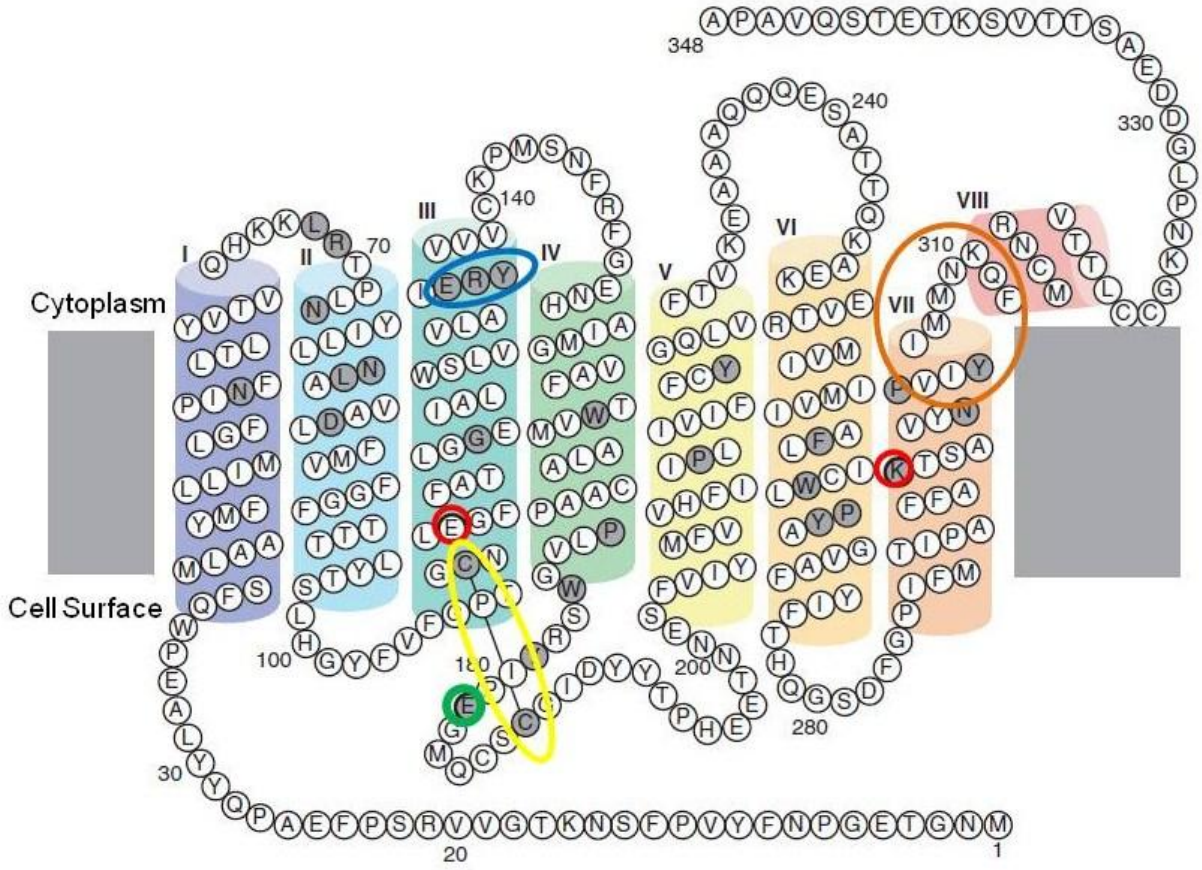

Figure 1-5: Structure of bovine Rhodopsin

Here a schematic representation of bovine Rhodopsin as described in 2000 is shown (36). A functional photoreceptor consists of seven transmembrane helices with a conserved cytoplasmatic C-terminal stretch (highlighted in orange), two Cysteine residues that form a disulfide brigde (shown in yellow) and the highly conserved Lysine K296 for chromophore binding and its counterion at postion 113 (E113), highlighted in red. In some opsin families this counterion is shifted to position 181 (shown in green). The characteristic transducin binding domain is highlighted in blue. Figure adapted from (19).

Besides the Lysine residue and the counterion D113 or E181, a transducin binding domain in helix III is higly conserved. This domain has the characteristic sequence ERY in TMT-Opsin families A and C and in Encephalopsin. For the TMT-Opsin family B this sequence is DRY (19, 27).

This difference in binding residues implicates a functional divergence between the different families. Apart from the above mentioned, two cystein residues (C110 and C187) that form a disulfide bridge necessary for stabilistaion of the protein are highly conserved throughout all Opsin families (37).

TMT-Opsins and Encephalopsin exhibit the structural features that are necessary for a functional photoreceptor (Figure 1-3, 1-4). This strongly indicates that these opsin families are indeed functional photoreceptors and good candidates for preceiving photic information and regulating light induced reflexes.

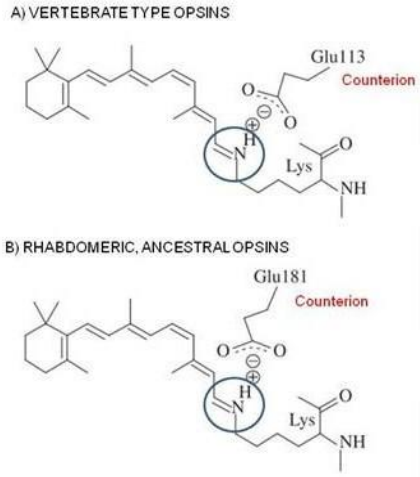

Structural feature	TMT-Opsin A	TMT-Opsin B	TMT-Opsin C	Encephalopsin
7 TMD	conserved	conserved	conserved	conserved
Schiff Base	K296	K296	K296	K296
Difulfide Bond	conserved	conserved	conserved	conserved
Counterion	E181	E181	E181	D113/E181
Transducin BD	ERY	DRY	ERY	ERY

Figure 1-6: Structural characteristic of photoreceptors in TMT-Opsins and Encephalopsin

On the right hand side the highly conserved domains important for the functionality of a photoreceptor as present in Encephalopsin and TMT-Opsins are summarized. On the left the structure of 11-*cis*-retinal is shown (picture from (20)). It is coupled to the protein component via a protonated Schiff Base linkage that requires a negatively charged counterion for stabilization. In Encephalopsin and in rhabdomeric type, more ancient, opsins this counterion is present at postion 181. In ciliary, vertebrate type opsins this counterion is most often shifted to a glutamate at position 113 (Table adapted from (27).

1.5 Model organisms

Zebrafish (*Danio rerio*) and Medaka fish (*Oryzias latipes*) are well-established model organisms in a variety of fields in biological research. These teleost fish are small in size and can easily be cultivated at relatively low cost. For both species a number of tools are well available such as the generation of transgenic lines, targeted knock-outs or *in situ* hybridization techniques. Besides that, the genome sequence of both animal models is easily accessible (38) and for Zebrafish genomic, gene expression, anatomical and developmental data are freely available from the Zebrafish Information Network ZFIN (39).

The comparison of gene expression and regulation between Zebrafish and Medaka is especially interesting from an evolutionary point of view. The last common ancestor of these species lived about 115-200 million years ago (40). This relatively large phylogenetic distance makes these model organisms very good candidates to study conserved as well as divergent mechanisms of gene regulation and expression. After a fish specific genome duplication event teleostei evolved independently from each other (41). So did the duplicated genes by either loss of function (nonfunctionalisation), neofunctionalisation or subfunctionalisation, i.e. both copies of the gene are mutated to the point where the original function of the gene can only be carried out if both complement each other (42-43). The comparison between those paralogues makes it possible to draw conclusions on how genetic and biochemical regulatory mechanisms diverged also in other vertebrates where no duplication occured and on what the ancestral function of the homologous genes might be (42).

In the context of chronobiology another advantage in choosing the two teleost species has to be mentioned. As a tropical freshwater fish indigenous to the Indian subcontinent Zebrafish are not subjected to non-tropical seasonal influences. However they do exhibit a reproductive behavior mediated by photoperiod and spawning has been observed at dawn in the laboratory as well as in the wild (44). Medaka on the other hand is native to Korea, Japan and Eastern China (45) where a seasonal variation in day length and temperature occurs. Medaka has been shown to display a seasonal reproductive behavior driven by light and temperature differences (46).

This allows us to study the involvement of deep brain photoreceptors in seasonal breeding in *Oryzias latipes* and the possible role of TMT-Opsins and Encephalopsin in photoperiodic time measurement looking at conserved features as well as differences in gene expression and function between the two teleost species.

1.6 The goal of my project

The two teleost species *Danio rerio* and *Oryzais latipes* possess a wide spectrum of Multiple Tissue Opsins. However little is known about their biological role. The primary goal of my project is to further characterize these photoreceptors. For this I analysed the expression pattern of different Multiple Tissue Opsins via whole mount *in situ* hybridisation to determine differences in patterns dependent on light stimuli and developmental stages. Furthermore I assessed non-visual Opsin expression in the eye of both larval Zebrafish and adults. Given that more data on TMT-Opsin expression exists for Medaka, here the focus of my experiments was on the Zebrafish homologues. Additionally I compared the expression patterns of different classes of non-visual Opsins in the deep brain of Zebrafish.

Besides that I was working toward the establishment of an *in vivo* approach to investigate their physiological function in transgenic reporter lines in Zebrafish and knock-out mutants in Medaka. In this context I identified a functional Zinc Finger Nuclease for Medaka *tmtopsb* to be employed for the generation of knock-out lines, that can be used for functional analyses.

I also established a BAC (Bacterial Artificial Chromosome) recombineering pipeline to modifiy BACs that carry the genomic locus of a respective TMT-Opsin for the establishment of transgenic reporter lines. This serves two goals. First it allows us to identify expression domains and photoreceptor cell types by visualising them via EGFP labelling. Secondly a bacterial Nitroreductase (NTR) is contained in the transgenic construct. This can be used for targeted cell ablation and therefore the investigation of the physiological role of the photoreceptors.

2 Methods and Material

2.1 Fish Culture

All fishes were kept in freshwater tanks at 26ºC under normal light conditions with a 14 hours light/10 hours dark cycle. Zebrafish embryos for injections or *in situ* hybridizations were obtained by setting up crosses in standard breeding tanks. Those tanks contain an insert with a special wall surface and slits in the bottom allowing the eggs to fall through and easily be collected. Since the onset of light in the morning is a major stimulus to induce mating, couples were generally set up in the late afternoon. For all experiments offspring of AB and Tüb wildtypes or mitfa, a mutant strain lacking pigmentation, were used. Medaka embryos were collected from the CAB inbred strain. Fishes were kept in mating tanks with three females and one male per tank. The embryos were obtained by scraping the egg clutches from the female's belly with a small hook. Embryos were raised in petri dishes in 1xE3 (Zebrafish) or 1xERM (Medaka) and set out after approximately 7 days, i.e. after they started swimming. Larval fish were first fed with dust food, the diet was then switched to dust food and artemia for larval fish and later on artemia and flake food for juveniles and adults.

2.2 BAC Transgenesis

In general Bacterial artificial chromosomes (BACs) can hold genomic segments with a size of up to 300kb and have become a well established tool in the creation of transgenic animal models and the analysis of gene function and regulation (47). Since the whole genomic locus of a gene of interest can be comprised within the BAC, distal and *cis*-regulatory elements are contained in the genomic segment, in contrast to plasmid based transgenic constructs where not all regulatory elements necessary for the spatial and temporal expression profile of the gene of interest may be included.

Here BACs for *tmtopsa1*, *tmtopsb1*, *tmtopsb2* and *encephalopsin* were modified in a way that a recombination cassette carrying *egfp* (enhanced green fluorescent protein) or *egfp* in combination with a bacterial nitroreductase (*ntr*) was inserted into the genomic sequence thereby replacing the first exon of the *opsin* gene.

EGFP expression under the control of the endogenous enhancer elements allows for the observation of the expression pattern *in vivo*, bacterial nitroreductase catalyses the conversion of metronidazole, a prodrug that can be added to the fish rearing medium, to a cytotoxic agent inducing targeted apoptosis of the opsin-expressing cells (48).

2.2.1 Identification of BAC clones for *tmtopsa1*, *tmtopsb1*, *tmtopsb2* and *enc*

BACs harbouring the genomic locus of the respective opsin genes of interest were identified by BLAST searches on the EnsEMBL genome browser (http://www.ensembl.org/Danio_rerio/) (38) (Appendix 6.2.). For all Zebrafish opsins mentioned above BACs from the BACPAC Resource Center CHORI-211 library were chosen. Here the genomic sequence derived from Tüb males, from the testis, and had been cloned into the vector pTARBAC2.1 and transformed into the bacterial strain DH10B [http://bacpac.chori.org]. Bacteria carrying the BAC were streaked out on selective LB plates containing 15mg/ml chloramphenicol (Sigma). The integrity of the BAC was checked via colony PCR with nested primers located approximately 100bp upstream and downstream of exon 1 of the respective *tmtopsin*. The upstream and intronic sequences were extracted from EnsEMBL and primers were designed using CLC Bio Main Workbench 5.7.1. Colony PCR was performed using FirePol Taq from Solis BioDyne with a standard 25µl reaction as described in the manual and with the following cycling conditions: denaturation at 95°C for 2 minutes, 30 cylces with 10 seconds denaturation at 95°C, annealing for 20 seconds at 58°C, elongation at 72°C for 45 seconds and another elongation step at 72°C for 10 minutes. The reactions were stored at 10°C until futher analysis. In the case of *tmtopsb1* and *tmtopsb2* the Qiagen HotStartTaq polymerase was used for colony PCR according to the manual in a 25µl reaction with the following PCR program: 95°C for 5 minutes for denaturation and activation of the polymerase, 29 cylces with 95°C for 20 seconds, annealing at 62°C for 30 seconds, elongation at 72°C for 50 seconds and again for 10 minutes and storage at 10°C.
5µl of each reaction were analysed on a 1% agarose gel run at 120V and one positive band each was gel-eluted on a SYBRsafe agarose gel with the Qiagen DNA extraction kit. The fragment was checked by sequencing with the respective inner nested primer.

2.2.2 BAC recombineering

In the course of this project three different approaches for BAC modification through holomogous recombination were carried out.

On the on hand the recombineering pipeline was performed using a Counter-Selection BAC Modification Kit (Gene Brigdes, www.genebridges.com). This system relies on the fact the the bacterial strain DH10B which carries the BAC is resistant to streptomycine because of a chromosomal mutation of *rpsL* encoding the ribosomal protein S12 (49). For counter selection a cassette conferring streptomycine sensitivity is inserted into the BAC, replacing exon1 of the respective *tmtopsin*. Positively recombined clones are identified through a growth control on selective LB plates with 3µg/ml tetracycline (Sigma), 15µg/ml kanamycine (Sigma) and 50µg/ml streptomycine (Sigma). Streptomycine-sensitive clones can be used for a second recombineering step where the *rpsLneo* cassette is replaced by a non-selectable cassette encoding EGFP-NTR-SV40 (E2N). The bacteria that loose the *rpsLneo* cassette in this step should regain their streptomycine resistance and positive clones can be selected on LB-plates containing streptomycine and chloramphenicol.

Here however streptomycine resistance was not efficiently conferred and multiple BAC species were identified in the modified bacteria.

In the case of *encephalopsin* colony PCR using flanking primers that bind outside of the recombination cassette was performed after the second recombination step using Qiagen HotStarTaq as described above with an elongation time of 2 min 10 seconds. The PCR showed bands at approximately 520 bp, corresponding to *enc* exon 1, at app. 1,5 kb corresponding to the inserted *rpslneo* and at 1,9 kb corresponding to inserted E2N. The insertion of the E2N cassette was again confirmed by colony PCR with a forward flanking primer and a reverse primer binding within *egfp*. In order to separate the different BAC species mini preps of 15 clones were performed according to an alkaline lysis BAC mini prep protocol.

These clones were again tested via colony PCR and one positive BAC was used for re-transformation into Top10 electrochemically competent cells (Invitrogen) by electroporation and plated on LB-chloramphenicol-streptomycine in order single out individual BAC clones. The bacteria were then replica-plated onto chloramphenicol-streptomycine and chloramphenicol- kanamycine with a velveteen stamp for a growth control.

Bacteria that did not grow on kanamycine were tested via colony PCR and one clone was prepped and analysed in an analytic digest with XhoI (NEB) on a 0,8% agarose gel in comparison to the wildtype and the *rpsLneo* positive BAC.

In order to avoid these screening steps, a new approach was tested. A cassette encoding EFGP-SV40 fused to *rpsLneo* was constructed and integrated successfully into the BAC containing the genomic locus of *tmtopsa1*.
We chose *rpsLneo* as a marker since here the promoter under which the selection marker neomycine is expressed is designed for expression from a low-copy BAC and confers antibiotic resistance even at a low gene dosage. In two PCRs the two parts of the fusion construct were amplified using the Finnzymes Phusion polymerase in a 50 µl reaction according to the manufacturer's manual with HF Buffer and a two step program with 98º C for 2 min, 5 cycles with 98 º C for 15 seconds, annealing at 62 º C for 30 seconds, elongation at 72 º C for 50 seconds and another 29 cycles with an annealing temperature of 66 º C. The EGFP-SV40 fragment was amplified from the vector EGFP-N1 with a forward primer binding 20bp upstream of *egfp* and a reverse primer binding downstream of the SV40 polyA signal with a 23 bp overhang complementary to the *rpslneo* 5' end. *rpsLneo* was amplified with a fusion primer carrying a 28 bp overhang complementary to SV40 at it's 5' end and a reverse primer binding at the 3' end of *neomycine*. The 1 kb and 1,3 kb sized fragments were gel-eluted in 30 µl and for the fusion PCR. 1 µl of a 1:10 dilution of each fragment was used as template in a 50 µl reaction with FusionTaq polymerase and HF buffer. The PCR was performed with 30 cylces, annealing at 68 º C for 30 seconds and 50 seconds elongation with a nested forward primer and the same reverse primer for *rpsLneo* as used previously.

The 2,3 kb fragment was gel-eluted and subcloned into the vector pJet2.1 with the Fermentas CloneJet Blunt-End cloning kit as described in the manual and transformed into One Shot Top10 competent cells (Invitrogen) using 5 µl ligation mix per 25 µl bacteria. Positive clones were selected on LB-Amplicilin plates and the vectors were tested by EcoRI (Fermentas) as well as AfflII (Fermentas) digestion and sequenced with pJet for and pJet rev (LGC Genomics).

For FastDigest restriction digestion generally 1 µg DNA was used in a 20 µl reaction and incubated at 37º for up to 45 min. For recombineering the subcloned fusion construct was used as a template for amplification of the recombination cassette as described in the Appendix (Appendix 6.3.).
This cassette was used for recombination into zC41F6.ya carrying *tmtopsa1* via pRedET-mediated integration. Integration was analysed via colony PCR and all positive clones were grown in liquid culture in LB-kanamycine overnight to loose the wildtype BAC. After this was confirmed with another PCR, positive clones were checked in an analytic digest with AfflII and sequenced with primers binding in the BAC genomic region upstream of the cassette and within the SV40.

For *tmtopsb1* and *tmtopsb2* another vector served as template for the recombination cassette (courtesy of Mihail Sarov). Here the rpsLneo gene is flanked by two FRT (Flip Recombinase Target)-sites, recognition sites for a flippase that is espressed under an inducible promoter (50-51). The flippase as well as phage lambda derived recombination proteins under an L-Rhamnose-inducible promoter are encoded on the vector pRedFlp4.The flippase is expressed in the presence of anhydrotetracycline (AHT) (Sigma). It specifically recognises the FRT sites and excises the selection marker, which can easily be checked via growth control on kanamycine plates and colony PCR.
The vector that serves as template for the homology cassette possesses an R6K origin of replication, which requires the *pir*-encoded protein pi in oder to replicate (52). This means that the plasmid carrying this origin of replication can only be propagated in pir+ E. coli. Hence the risk of vector contamination from residual template and false-positive clones when transforming DH10B competent E. coli with the recombination cassette is eliminated.
pRedFlp4 can be selected on Low Salt LB plates containing 100 µg/ml Hygromycine B (Sigma) or LB-plates containing 200 µg/ml of the antibiotic. The BAC for *tmtopsb1* (zC226G17.ya) was transformed with a cassette encoding *E2N* and *rpsLneo* flanked with FRT sites and *tmtopsb2* (zC161K7.za) with a cassette carrying EGFP-SV40 and the flanked *rpsLneo*. For the latter the resistance marker was flipped out by growing the bacteria over night in liquid culture in the presence of anhydrotetracycline (AHT) until the culture was saturated. From this 10 µl were used for inocculation of fresh media with AHT and chloramphenicol.

The bacteria were again incubated for approximately 8 hours. Flipping was checked via colony PCR and growth control on selective plates. Positive clones were sent for sequencing. Figure 2.1 shows an overview over recombination cassettes used in the course of this project.

For *tmtopsa1* an additional cassette was recombined into the BAC. Here *mcherry* is expressed under a heart specific cardiac myosin light chain 2 (cmlc2) promoter and acts as transgenesis marker.

This promoter is active in all myocardial cells and Zebrafish larvae in which the transgene is expressed from the injected BAC can easily be identified by screening for their red fluorenscent – "bleeding" – heart (53).

The *clmc2: mcherry* cassette was integrated into the 3' end of the TMT-OpsinA1 encoding BAC via RedET facilitated recombination. An ampicilin resistance gene served as selection marker for this cassette.

For injections BACs were Maxi-Prepped according to the Qiagen Maxi Prep Columns Tip 500 protocol from 250 ml cultures with the following changes: resuspension in 15 ml P1 shaking for 10 minutes at 37ºC, lysis with 15 ml P2, neutralisation in 15 ml P3, spinning for 70 minutes at 4000rpm, elution with 15 ml QF (endotoxin-free) warmed up to 65ºC, precipitation and subsequent washing in 70% ethanol for 90 min at 4000 rpm each and resuspension in 250- 300 µl. This usually yielded between 300 to 500 ng/µl DNA (protocol from David Keays, personal communication). Before injection the Maxipreps were checked in an analytic digest for contamination with genomic DNA.

2.2.1 Bac Injections

The recombined BACs were injected into one or two-cell stage Zebrafish embryos. For this couples were set up in mating cages on the day before the injection. Male and female were kept apart with a plastic insert in the cages and by removal of this separator in the morning mating was induced. Eggs could be collected after approximately 30 minutes in petri dishes filled with 1x E3. The injection solution was prepared in the meantime.

Here 150 ng/µl -250 ng/ µl BAC DNA was coinjected with a homing endonuclease PI-*Sce*I (NEB) that linearises the BAC backbone, and 1x NEBuffer in a total volume of 20 µl. Linearization of the injected DNA has been show to increase the efficiency with which the BAC is integrated into the genome (54). Generally 0,5 µl TRITC was added to the injection solution.

For *tmtopsa1* no injection marker was used so *mcherry* expression could be detected more easily. Injected embryos were raised 1xE3 at 28ºC and screened for fluorescent protein expression under the Zeiss Stereo Lumar. See appendix 6.4 for a detailed microinjection protocol.

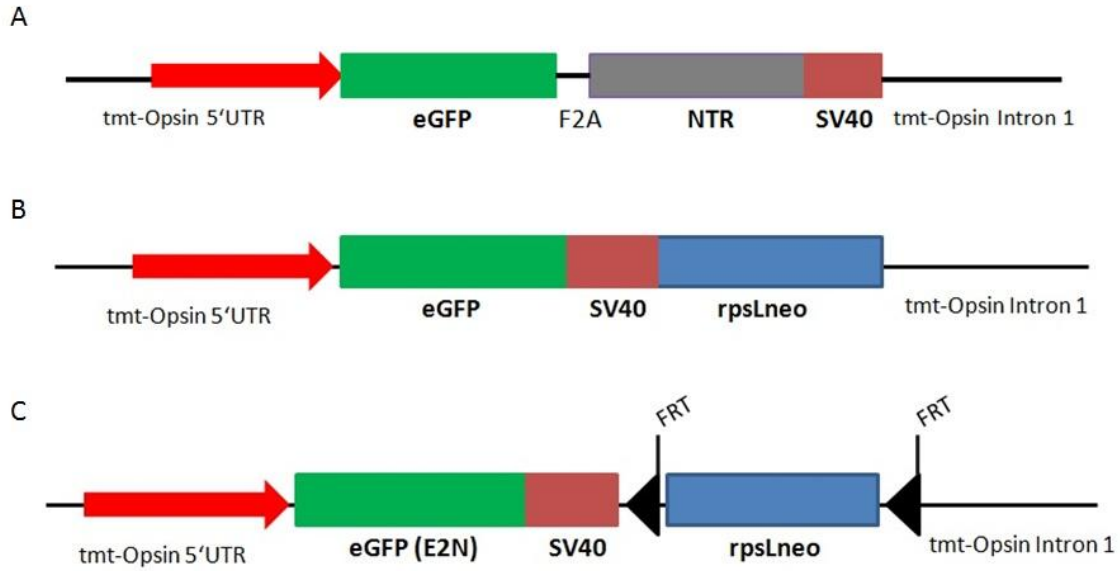

Figure 2-1: BAC Recombineering Transgenes for tmtOpsinsA1, B1, B2 and Encephalopsin

A A non-selectable cassette was used to replace *encephalopsin* exon 1 via a two step procedure using the GeneBridges Counter Selection Kit
B Fusion contruct used to visualize *tmtopsa1* expressing cells. *rpsLneo* acts as selection marker in the recombineering process.
C Flanking rpsLneo with FRT sites allows for the excision of the selection marker by induction of flippase-expression after integration of the cassette in the BAC. For t*mtopsb1* an eGFP-F2A-NTR (E2N) cassette was constructed, for *tmtopsb2* a cassette encoding only eGFP was used.
eGFP – enhanced green fluorescent protein; F2A – ribosomal skip site; NTR – bacterial nitroreductase

2.3 Targeted knock-out of Medaka TMT-Opsins using engineered Zinc fingers

Targeted gene knock-out facilitated by engineered zinc finger nucleases (ZFNs) is a well established tool in zebrafish mutagenesis (55-56). This system relies on the fact that arrays consisting of three of more individual zinc fingers can be assembled from archives of pre-selected ZFN domains to specifically recognize a target sequence within the gene of interest [14]. A zinc finger is a DNA binding motif found in a number of transcription factors with a characteristic structure where a stabilizing Zn^{2+} ion is coordinated by two cystein and two histidine residues (57). For genome editing three or more individual Cis_2His_2 zinc finger domains are fused to the cleavage domain of the type II restriction enzyme FokI (58). FokI is a heterodimer that introduces a double strand break (DSB) into DNA upon dimerization (59).

Introduction of DNA lesions requires two 9 bp zinc-finger-binding sites that are located within close proximity of each other with an approximately 6 bp spacer in between (60) (Figure 2.2).

Upon binding of the ZFNs to the target site dimerization can occur and FokI cuts within this spacer region and produces a DSB. This will be fixed by the cellular non homologous end joining (NHEJ) repair machinery (14-16). This repair mechanism in relatively prone to create errors in the DNA, such as small insertions or deletions that can cause a frame shift in the coding sequence and lead to the occurance of a premature stop or a nonsense mutation [14]. Assembly of ZFN targeting Medaka *tmtopsa1* and *tmtopsb*, injection of the ZFN-RNA into one cell stage Cab embryos and screening for ZFN-induced genetic lesions will be described in the following.

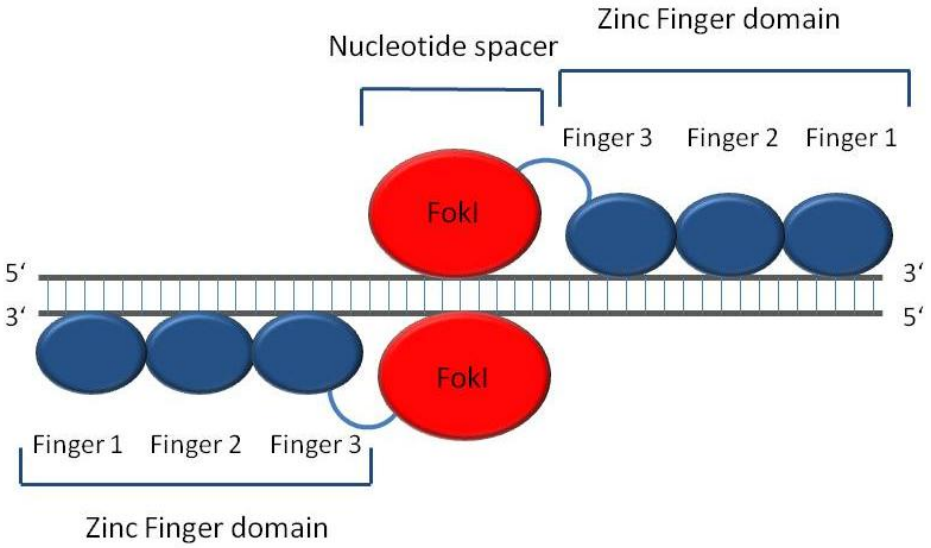

Figure 2-2 Gene targeting using engineered zinc finger nucleases (ZFN)

Arrays of three individual zinc fingers can be assembled to specifically recognize a 9 bp sequence within the gene of interest and fused to FokI nuclease heterodimer variants. Upon binding of the ZFN to its target sequence dimerization can occur and the nuclease introduces a double strand break in the DNA. This will be mended by the cell's endogenous DNA repair machinery via non-homologous end joining (NHEJ). NHEJ is an imperfect repair mechanism and may result in the introduction of insertions or deletions which can ultimately cause a frame shift in the coding sequence and silencing of the respective target gene. (Figure adapted from (58))

2.3.1 Assembly of ZFN targeting O.l. *tmtopsa1* and O.l. *tmtopsb*

The cDNA sequences of *tmtopsa1*and *tmtopsb* were screened for ZFN target sites *in silico* using a zinc finger target site algorithm (Scot Wolfe, http://pgfe.umassmed.edu/ZFPsearch.html). For each gene 2 pairs of three-finger zinc finger proteins (ZFPs) were selected with target sites located in exon 1 (*tmtopb*) or exon 2 (*tmtopa1*) distal from exon-intron boundaries (sequences from Ruth Fischer) (Appendix 6.5.).

The individual fingers were amplified from template vectors provided in a ZF Consortium Modular Assembly Zinc Finger Set (Addgene, Keith Joung) in a standard 15 µl Phusion polymerase reaction (Finnzymes) using HF buffer and Zinc finger specific primer pairs ZFP1, ZFP2 and ZFP3 for the respective ZFP domain.

The following PCR programs were applied: 98ºC for two minutes, 24 cycles with 94ºC for thirty seconds, 68ºC for thirty seconds, elongation at 72ºC for 20 seconds and storage at 10ºC for ZFP1. For ZFP2 and ZFP3 the program was changed to 19 cycles with an annealing temperature of 57 ºC.

1,5µl of each PCR product were then directly used in an overlapping PCR with five cylces with 98 ºC for 2 minutes, 94 ºC for 30 seconds and 72 ºC for 30 seconds. After this the program was paused to add 4 µl each of ZFP1 forward and ZFP3 reverse primer and clycling was resumed with 24 times 98ºC for 15 seconds, 68 ºC annealing for thirty seconds, 72ºC elongation for thirty seconds and storage at 10 ºC.

In the following the PCR fragments were eluted on a 2% agarose-metaphor gel. Metaphor is a form of agarose with a high resolution capability which allows to distinguish even very small bands on the gel. The eluted bands were digested with BamHI (Fermentas) and Acc65I (Fermentas) and cloned into the equally cut and dephosophorylated (Antarctic Phosphatase, NEB) FokI expression vector in a 1:7 vector to insert ratio using T4 ligase (NEB). 5' ZFPs were cloned into the vector pCS2-Flag-DD-FokI (stock number 584) while the 3'ZFPs were ligated into pCS2-Flag-RR-FokI (stock number 585), both encoding the respective nuclease variant. After transformation positive clones were selected via colony PCR with two primer sets: ZFP1 foward and ZFP3 reverse as well as a primer pair amplifying only the insert contained in the undigested vector, to exclude the occurance of false-postives due to contamination with undigested vector. Besides that the cloning was verified via sequencing with Sp6.

For the *in vitro* transcription all vectors were linearized with NotI (Fermentas) and mRNA was synthesized using the Ambion mMessage mMachine Kit with Sp6 RNA polymerase. During this procedure a 7-methyl guanosine cap is added to the 5' end of the mRNA so it can directly be translated *in vivo,* in the injected embryo. RNA was purifired using the RNAeasy Mini Kit (Qiagen) and standard RNA Cleanup protocol, eluted in 30 µl RNAse-free ddH_2O and stored in 5µl aliquots at - 80ºC.

2.3.2 Injection of ZFN mRNA into one-cell stage Medaka embryos

For the injections males and females of the Cab strain were separated over night and set back together in the morning.

Fertilized eggs could be collected approximately 30 – 40 minutes later by scraping them off the female's belly with a small hook. The eggs were separated from each other by rolling them gently in the collection dish filled with pre-cooled 1x ERM.

Since Medaka are not sensitive to low temperatures the dishes with the embryos were kept on ice to slow down the embryonal development. Injections were started at a low mRNA concentration with 10 ng/µl per ZFP and slowly increased to a total of 60 pg injected into each embryo. The injection mix contained the mRNA of each ZFP, 0,5µl TRITC (Tetramethylrhodamine-5-(and 6)-isothiocyanate) per 20 µl solution and RNAse-free H_2O. The injection volume was estimated according to the embryo's size and calculated with the following equation: $V[\mu l]=\frac{4}{3} \times \pi \times r^3$ to account for approximately 0,5 nl per embryo. The embryos were sreened using the Zeiss StereoLumar and all injected ones were frozen in liquid nitrogen at two days post fertilization.

2.3.3 Analysis of genome editing in the ZFN target site

In order to assess whether genome editing had occurred at the ZFN target site genomic DNA was extracted from two day old embryos using the Nucleospin Tissue kit from Macherey-Nagel.

DNA extraction was performed according to the manual with the only change that the embryos were mashed using plastic pistils before pre-lysation, to break the relatively thick chorions and allow a complete lysis by proteinase K digestion.

The genomic DNA was scanned for mutations in the ZFN target site using the Applied Biosystems HRM (High Resolution Melting Curve) Software v2.0.

Here a 150bp fragment containing the ZFN target site is amplified in the presence of a fluorescent dye (MeltDoctor HRM Dye, Applied Biosystems) that specifically binds doublestranded DNA and emits a fluorescent signal only in its bound form. Melting of the PCR amplicon results in a release of the dye and decrease in fluorescence, which can be measured.

The melting temperature for each fragment depends on its sequence, length and GC-content, so mutations within the amplicon can be determined by comparison of the melting curves between wildtype and presumptive mutants.

In order to test the resolution ability of the software a construct was made with a 30bp deletion compared to the wildtype *tmtopsb* ZFN target site.

The fragment was cloned via a standard two-step fusion PCR using Finnzymes Phusion polymerase in a 50 µl HF-Buffer reaction and the *tmtopsb* ZFN target site subcloned into pBKS-CS (stock number 811) as template.

This also served as template for the HRM analysis, as well as the deletion construct subcloned into pJet2.1 and genomic DNA extracted from two day old injected embryos and wildtype larvae at 10 ng/reaction and 20 ng/reaction. The HRM reaction was performed using the Applied BioSystems StepONEPlus Real Time PCR System.

2.4 Whole Mount *In Situ* Hybridisation

Whole Mount *In Situ* Hybridisation was employed to analyse and compare the expression patterns of multiple tissue opsins in Zebrafish larvae. For this the fish were fixed at 3 dpf or 7 dpf. PTU (Phenylthiourea), an inhibitor of the enzyme tyrosinase was added to the rearing medium 1dpf to inhibit pigmentation and allow a better observation of the stainings (61). Besides that larvae that developed under normal light conditions with 14h light and 10h darkness were compared to ones that were incubated in complete darkness, where the culture dishes were wrapped in aluminium foil. For fixation the rearing medium was replaced by 4% PFA/1xPTW and the larvae were incubated in the fixative over night at 4ºC. The PFA was then removed, the fish were washed in 1x PTW and stored at -20 ºC in 2ml Eppendorf Tubes in 100% Methanol, which denatures the cell membranes, for a minimum of 30 minutes.
After this the fixed larvae were rehydrated step by step by washing them 5 minutes each in 50% MeOH, 25% MeOH and twice in 1x PTW on the shaker.
In order to make the tissue accessible for the RNA probe and to remove ribosomal proteins from the target mRNA the samples were digested with 10µg/ml proteinase K in 1x PTW for 30 minutes at room temperature.

The digestion was stopped by adding 2mg/ml glycine and the samples were post-fixed at room temperature for 45 minutes, before washing them three times in 1x PTW and incubating them for 1 hour in Hyb+ hybridization mix at 65 ºC. After this the digoxigenin-labeled antisense probes were added.

RNA probes were generally prepared from the vectors pJet2.1 or pGemT-easy carrying the respective *tmtopsin* cDNA (cloning done by Stephan Kirchmaier or Ruth Fischer). The antisense RNA probe was transcribed either from T7 or SP6 promoter.

For this 5µg of the vector was linearized using a restriction enzyme that cuts at the 5'end of the inserted cDNA sequence and eluted on a SYBRsafe gel using the Qiagen Gel Extraction Kit prior to the *in vitro* transcription.

In some cases due the orientation of the subcloned cDNA sequence it was necessary to add a promoter sequence via PCR with a reverse primer containig an Sp6 site and use the gel-eluted PCR fragment for transcription. For this to 10µl of the PCR product or digested vector 2µl of DIG-UTP dNTP mix or Fluo-UTP dNTP mix (Roche), 100mM DTT, 0,5µl RNAse inhibitor (Promega), 2µl Transcription buffer (NEB) and µl RNA polymerase (Sp6 or T7, NEB) were added and the mix was filled up to 20µl with RNAse-free water.

After incubation at 37ºC for up to 3 hours 1µl RNAse-free DNAse (NEB) was added and DNA was digested at 37 ºC for another 30 min before cleaning up the probes with the RNAeasy Mini Kit. The RNA was eluted in 50 µl RNAse-free water and its quality and concentration was checked in a 1% agarose gel. For this 3µl RNA were mixed with 6µl Formamide containing RNA loading dye and heated to 94ºC for 5 minutes to denature secondary structures before loading the samples on a gel. To the remaining eluat 75 µl Hyb+ mix were added and probes were stored at -20ºC and used for *in situ* hybridization in an appropriate dilution in Hyb+. For each sample 250µl of this dilution were heated up to 94 ºC for 10 minutes before using it to replace the Hyb+ mix in which the larvae had been prehybridized.

After 12 hours of hybridization at 65ºC the probe was taken of and the following washes at 65ºC were performed to remove any unbound RNA: 1x 5min in Hyb- (50% Formamide, 5x SSC, 0,1% Tween-20), 3x 10 min in 25% Hyb- (in 2x SSCT), 1x 5min in 2x SSCT, 2x 30min in 0,2x SSCT.

Then the samples were washed 1x 5 min in 50% 0,2x SSCT/ 50% MABT and 1x 5 min in MABT at room temperature and incubated for 1 hour in 1% DIG block (Roche) in MABT. After blocking the larvae were incubated in anti-DIG-AP for up to 4 hours at room temperature. The DIG antibody is coupled to an alkaline phosphatase that catalyses the conversion of a NBT/BCIP substrate BM purple (Roche) to a blue precipitate. Prior to adding the staining solution the samples were washed in MABT at 4ºC overnight and another 4 times for 15 minutes at room temperature. The staining was done in 24-well dishes in the dark and stopped with 1x PTW. The embryos were then post-fixed in 4% PFA and stored in 70% glycerol.

They were mounted on microscope slides in 70% or 100% glycerol for image acquisition using a Zeiss Axioplan 2 microscope. For double *in situs* with fluorescein-labeled probes against one mRNA and DIG-probes detecting the mRNA of another gene the samples were hybridized with a mix of both probes and washed as described above.

First the fluorescein-labeled probes were detected by incubation with anti-fluorescein-AP in a 1:1000 dilution in MABT. After incubation for 4 hours at room temperature the antibody was taken off and the samples were washed 4x 15 minutes in MABT and incubated in 0,1M Tris/HCl, pH 8,2 for 15 minutes. The washing solution was replaced with Fast red substrate solution (Roche, one FastRed tablet per 1 ml solution). The color reaction was stopped with 1x PTW and the samples were washed 3x 5 minutes in 0,1M Glycine/HCl, pH2,2; 0,1% Tween-20 to denaturate the phospatase. After another 4 washes in 1x PTW samples were incubated in DIG-block the detection of DIG-probes was continued as described above.

3 Results and Discussion

3.1. BAC Transgenesis

3.1.1 Establishment of a functional recombineering pipeline

The advantage of a transgene encoded on a BAC as opposed to a plasmid construct is, that here all regulatory elements needed for the expression of the gene of interest are available on the artificial chromosome. In the case of our Multiple Tissue Opsins the creation of transgenic lines serves two things. On the one hand *egfp* under the *opsin* specific promoter makes it possible to visualize the *opsin* expressing cells. On the other hand a gene encoding bacterial Nitroreductase (NTR) is included in the transgenic construct. This enzyme catalyses the conversion of a harmless prodrug metronidazole into a cytotoxic DNA-crosslinking agent (62). If metronidazole is added to the rearing medium of larvae expressing the transgenic contruct, NTR-positive cells will undergo apoptosis (63). This makes it possible to specifically ablate MTO-expressing cells and thus study the possible functions of these photoreceptors. BAC transgenes were constructed by homologous recombination as described above.

MTO	Transgene
enc	*e2n*
tmtopsa1	*egfp-rpsLneo cmlc2:mcherry*
tmtopsb1	*e2n-rpsLneo-FRT*
tmtopsb2	*egfp(-rpsLneo-FRT)*

Figure 3-1: Summary of recombined BACs

The table shows a summary of the recombined BAC clones that were obtained in the course of the project. The BAC encoding TMT-OpsinA1 was modified with a second cassette carrying *mcherry* as transgenesis marker. This second cassette encodes *mcherry* under the control of the heart specific promoter cmlc2 and expression of the transgene from the injected BAC can observed by screening the embryos for their red fluorescent heart. This BAC and the one for *tmtopsb2* were prepped and injected into one-cell stage zebrafish embryos (E2N- EGFP-F2A-NTR).

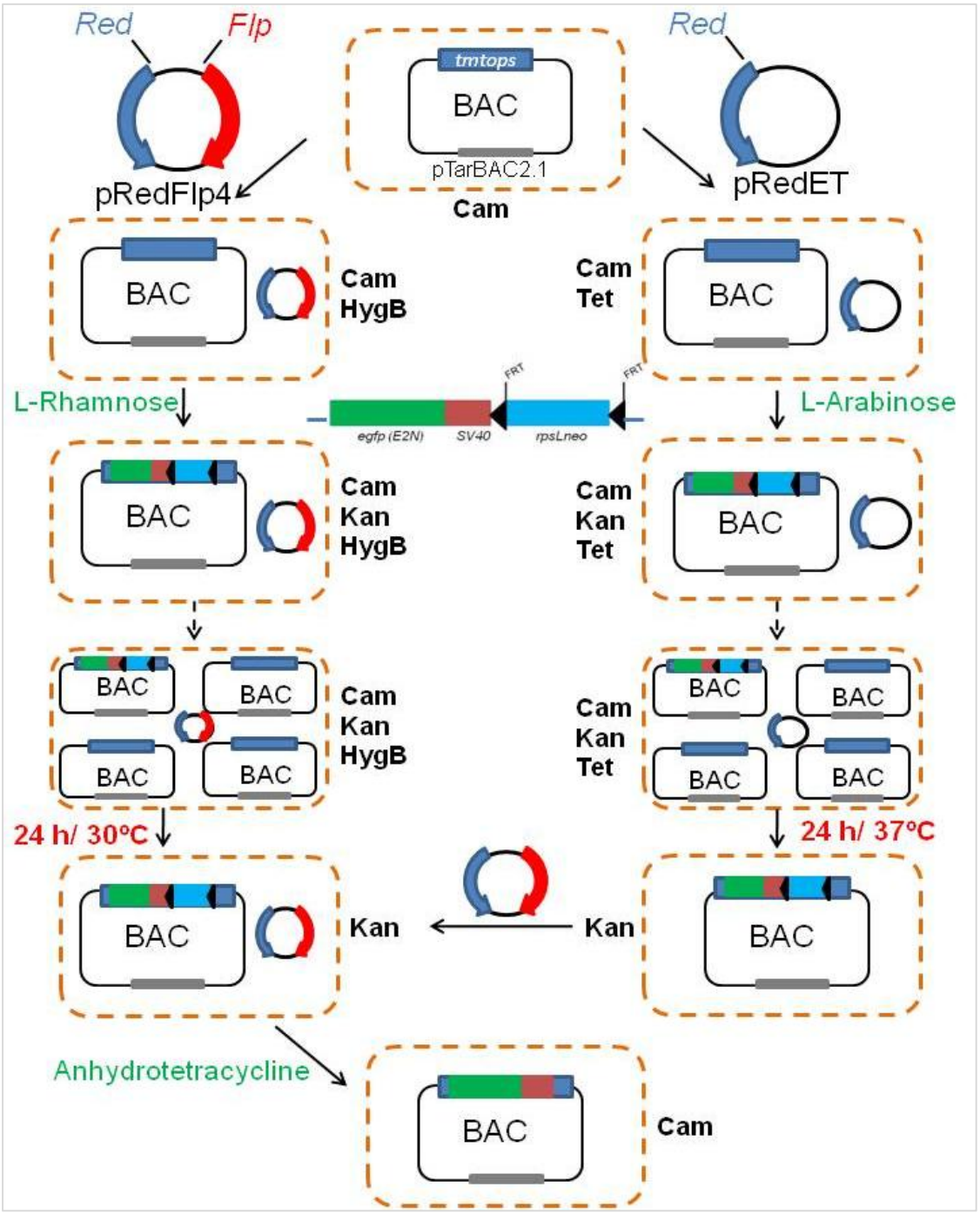

Figure 3-2: BAC recombineering pipeline

Here the two possibilities for BAC recombineering via homologous recombination are shown. Either the vector pRedET (GeneBridges) was used, or pRedFlp4 (courtesy of Mihail Sarov). Recombinases expressed from the vector under an inducible promoter mediated the integration of the homology cassette into the genomic locus. Since after this multiple BAC species seem to be present it is necessary to grow the bacteria in medium containing only the selection marker for the cassette, i.e. kanamycine. A flippase can be expressed from pRedFlp4 to excise the FRT-flanked selection marker.
Cam –Chloramphenicol, Flp –Flippase, HygB- HygromycineB, Kan- Kanamycine, Red – Redα/Redβ phage proteins, Tet – Tetracycline

Recombineering, i.e. recombination mediated engineering relies on the fact that doublestranded DNA fragments can be integrated into chromosomal stretches via homology regions as short as 50 bp utilizing a phage lambda derived recombination system Red/ET (64). Here phage proteins Redα and Redβ that catalyse the insertion of a recombination cassette replacing the genomic segment located between the two homology regions are expressed from a plasmid pRed/ET. pRed/ET contains the phage lambda redαβγ operon under the control of an L-Arabinose inducible promoter. The plasmid also carries a tetracyline resistance and a temperature-sensitive origin of replication allowing the tight control of the time frame in which recombination proteins are expressed to avoid unwanted rearrangements within the BAC or E. coli chromosome.

In the beginning BAC modifications were carried out using a two-step counter selection kit.

For this method however two problems arose. Streptomycine sensitivity was not efficiently conferred by the *rpsLneo* cassette and even though the bacteria were able to grow on kanamycine and colony PCR with flanking primers binding 3' and 5' outside of the cassette confirmed the insertion of *rpsLneo* at the correct location, selection for streptomycine sensitivity at most resulted in diminished growth. Only for the BAC zC246H18.ya carrying *encephalopsin* a streptomycine sensitive clone could be identified and used for the next step. However colony PCR showed multiple bands, that is a band at approximately 1,4 kb and a band at ca. 500 bp which is equivalent to the wildtype exon 1 of the the respective opsin (Figure 3.3).

This suggests the presence of multiple BAC species in the bacterial cells, even though BACs are generally maintained at a low copy number of one to two copies per cell (Figure 3.2.) (65). If the recombination cassette carries a selectable marker, such as *rpsLneo*, the wildtype BAC will be lost when the bacteria are grown over night in media containing only kanamycine. Without selection for chloramphenicol it will not be mantained in the cell and only *rpsLneo* positive clones will be obtained.

The fact the the bacteria were still able to grow on streptomycine despite carrying the *rpsLneo* cassette, conferring sensitivity to the antibiotic, most likely results from recombination between the endogenous – functional – *rpsL* and the integrated cassette. During the recombination procedure the vector pRedET remains in the bacteria for the second recombination step.

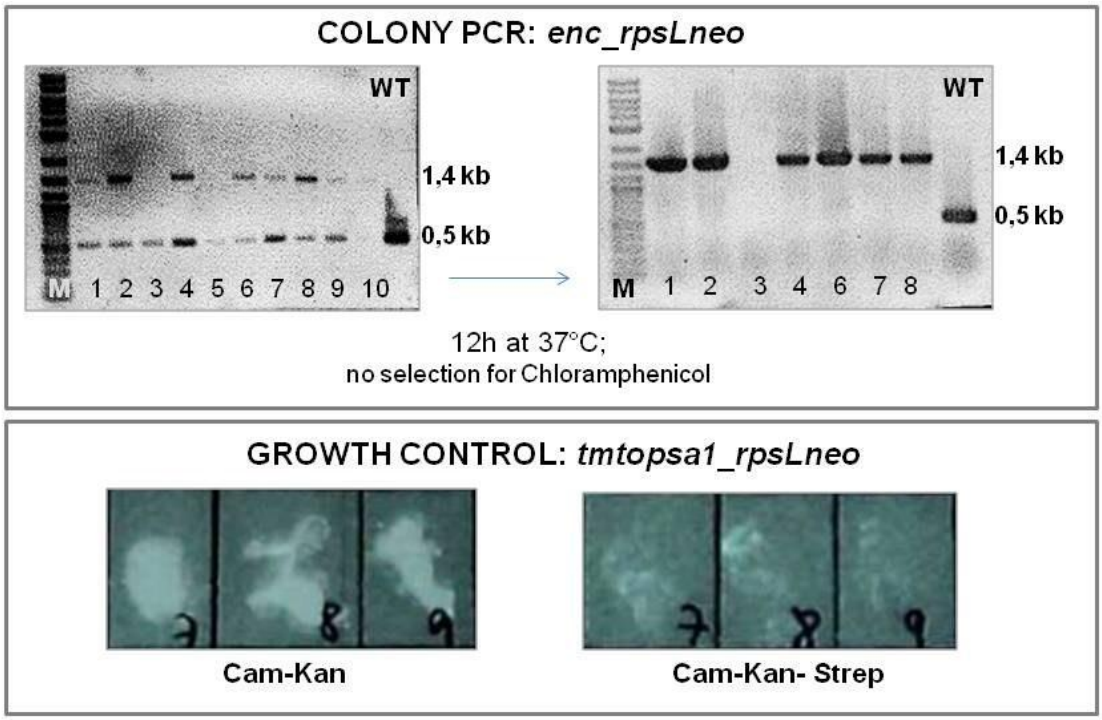

Figure 3-3: Representative colony PCR and growth control after transformation with *rpsLneo* cassette

The upper panel shows a colony PCR with primers flanking the first exon of *encephalopsin.* On the left 10 clones that had been transformed with the *rpsLneo* homology cassette replacing exon 1 were analysed. Two bands can be observed, one with a size of 1,4 kb corresponding to the inserted *rpsLneo* and one at 0,5 kb, the size of the wildtype *encephalopsin* exon 1. After growing several of the clones in liquid culture in the presence of Kanamycine and without selection for Chloramphenicol and repeated colony PCR, the lower band cannot be detected anymore. This shows that the wildtype BAC has been lost.
On the lower panel a growth control on selective LB plates with bacteria carrying the BAC encoding *tmtopsa1*, that had been transformed with the *rpsLneo* homology cassette, is shown. Here it becomes visible that even though the cassette must have been integrated into the BAC, conferring kanamycine resistance, the bacteria are still able to survive on plates containing streptomycine. Integration of *rpsLneo* at most results in diminished growth.
Cam- Chloramphenicol, Kan- Kanamycine M – 2-log DNA ladder (NEB), Strep- Streptomycine, WT- wildtype control

The inducible promoter araBAD however is not completely down-regulated in the absence of arabinose (66). This means that phage proteins are still expressed and can mediate recombination between the endogenous *rpsL* and the cassette. The presence of multiple BAC species in the cell on the other hand poses another problem to the procedure. Since the recombination cassette encoding the transgene is non-selectable, positive clones cannot be differentiated by mere selection on streptomycine – chloramphenicol plates. A selectable cassette consisting of a fusion between *egfp* and the selection marker *rpsLneo* was used to circumvent this problem.

If the selection marker is flanked by FRT sites, a flippase can be expressed from the vector pRedFlp4 that excises the marker. The recombineering pipeline that was established in the course of my project is shown in figure 3.2. The procedure was adapted from Sarov et al. (50-51)

3.1.2 Generation of reporter lines

For the generation of reporter lines the naked BAC DNA was coninjected with a homing endonuclease PI-SceI. This enzyme linerarizes the BAC backbone to facilitate integration into the genome. For BAC injections either Tüb or mitfa strains were used.
tmtopsb2:egfp-rpslneo(FRT) and *tmtopsa1*:*egfp-rpslneo/cmlc2:mcherry* were injected at concentrations of 150 -250 ng/µl. No *egfp* expression could be detected in the injected embryos. Only at 2 dpf *mcherry* was expressed from the TMT-OpsinA1-encoding BAC in 7 out of 30 injected embryos (Figure 3.4).
Generally the mortality of the injected fish was relatively high. This can either result from mechanical damage by the injection needle or a too high contamination of the BAC prep with bacterial genomic DNA.
The fact that green fluorescence was not observed can have several reasons. Possibly *egfp* expression in single photoreceptor cells is not detectable under the StereoLumar. Here it would be necessary to perform a genotype analysis to see wether integration of the transgene occurred. However the transmission of the integrated BAC might be to mosaic, so *egfp* expression in Multiple Tissue photoreceptors cannot occur.

A way to increase the integration efficiency and the probability with which the BAC is transmitted into the germline would be to include Tol2 sites into the construct. The Tol2 transposon is endogenous to vertebrate genomes and has originally been discovered in Medaka (67). Co-injection of a Tol2-flanked construct with Tol2 transposase mRNA facilitates a more efficient integration into the genome via these flanking sites (47). For transposition 200bp and 150 bp from the left and right ends of tol2 *cis*-sequences have shown to be essential and efficient for transposition of the BAC (68).

I constructed a cassette carrying these minimal sequences, *clmc2:mcherry* and an ampicilin selection marker for insertion into the BAC backbone (Figure 3.4). Using this cassette to integrate the transgenesis marker *mcherry* will increase the efficiency with which the BAC can be inserted into the genome.

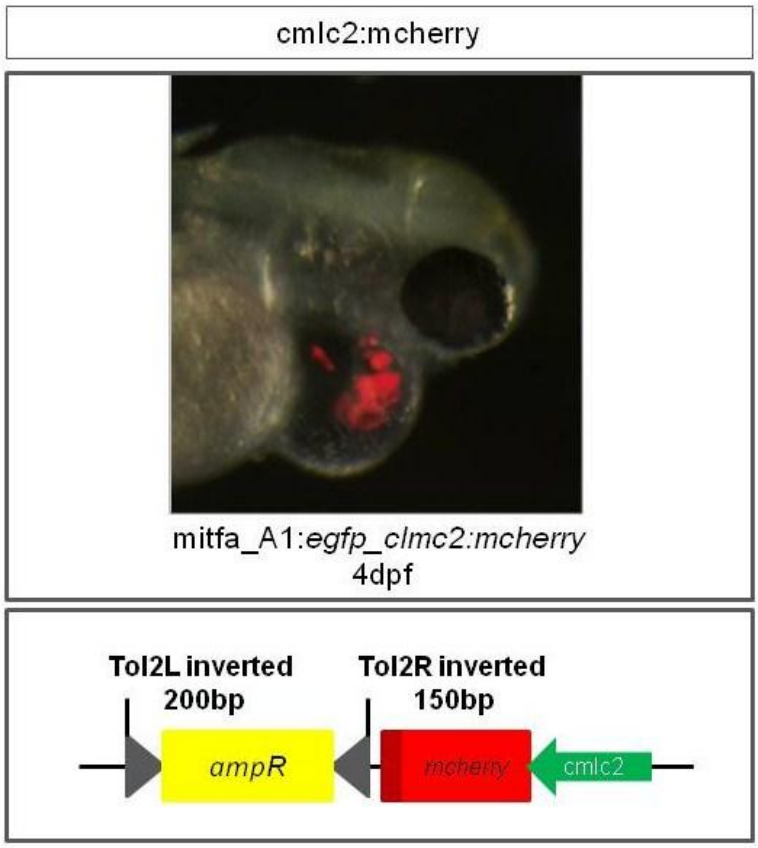

Figure 3-4: "Bleeding heart" – Expression of mcherry in Zebrafish larvae

On the top a 4-day old mitfa larva is shown in a lateral view with the anterior to the right. Expression of the transgenesis marker *mcherry* under the heart specific promoter cmlc2 can nicely be observed in the myocardium. On the bottom the piTol2 cassette carrying the minimal cis-sequences for functional transposition is depicted. This cassette can be integrated into the pTarBAC2.1 backbone via homologous recombination and will facilitate insertion of the modified BAC into the Zebrafish genome if co-injected with transposase mRNA.

3.1.3 Summary

Transposon-mediated BAC transgenesis is a well established tool for the generation of transgenic Zebrafish lines. Including Tol2 sites into the trangenesis marker should result in a more efficient transformation.
In order to verify the integration of the transgene genotyping PCR will have to be performed and *mcherry* expression analysis in the F1 generation will show whether a germline transmission occurred.

Visualization of MTO-expressing cell *in vivo* by EGFP labeling allows the identification of expression domains and characterization of the photoreceptor cell type. This will help to gain some insight into the functional implications of MTOs. For this cells can be isolated by laser microdissection or FACS (fluorescence activated cell sorting) and the cell morphology can be assessed in immunogold-labelled sections under the electron microscope.
Several classes of non-visual opsins have been shown to be expressed in the cerebrospinal fluid (CSF)-contacting neurons of the inner brain (11). Multiple Tissue Opsins are expressed in discrete areas of the central nervous system (CNS), that differ from already known photoreceptive sites. This raises the questions as to what extent the non-visual opsins share a common photoreceptor cell type, such as the CSF-contacting neurons and how the cell morphology differs between the individual families and MTO paralogues. Visualization of the neuronal projections that connect the photosensors to other tissues of the brain may lead to the indentification of cell types and functional implications of these opsins.

Functional studies will also be carried out by targeted cell ablation utilizing the NTR/Metronidazole system. This will allow to determine the physiological functions in which the MTOs are involved. Light-dependent mating behavior in Zebrafish (44) and seasonal breeding in Medaka (46) or the change of body color (69) and locomotor activitiy (70) can be analysed in transgenic lines. Given the high number of MTO family members it would be interesting to analyse whether their functions are also abundant, to what extent a neo- or subfunctionalisation of the different paralogues occurred and whether they can complement each other in their role as photoreceptor.

3.2 Identification of a functional Zinc finger Nuclease against Medaka *tmtopsb*

3.2.1 High Resolution Melting Curve Analysis

Zinc-finger Nuclease mediated mutagenesis has become a valuable tool in reverse-genetic approaches to determine gene function and regulation (71). While in Zebrafish this method of targeted gene knock-out (72) is very well established no publications exist on its use in Medaka so far. Zinc fingers that specifically recognize a target sequence can be assembled and fused to a FokI nuclease domain. The zinc finger nuclease will bind its target site and induce a lesion in the genomic sequence which can ultimately lead to a knock-out of the gene of interest (56, 73).

I cloned two Zinc Finger Nucleases for Medaka *tmtopsb* and *tmtopsa1* and injected the mRNA of the ZFNs targeting *tmtopsb* into one-cell stage embryos. At concentrations ranging from approximately 40 pg/injection volume to 80 pg/ injection volume for each finger a very high rate of misdevelopment and mortality could be observed in the injected embryos. This suggested that gene targeting and mutation occurred.

Initially read-out to analyse genome editing in the target site was carried out using a bacterial blue-white assay. The ZFN target site was amplified from genomic DNA extracted at 2 dpf and subcloned into a pBluescript vector in frame with β-galactosidase. If a mutation occurred in the injected embryos, functional β-galactosidase would not be expressed and the bacteria would show a white phenotype.

However this approach proved to be unreliable. Probably due to vector contaminations and problems during the ligation a very high number of white colonies proved to be false-negatives. The white and blue phenotype, respectively, appeared at what seemed a random distribution. PCR analysis and sequencing of clones carrying the potentially mutated Zinc Finger target site either showed no mutation or a nonsense insertion during the cloning procedure.

Therefore another approach was tested. Real-time PCR-based identification of genomic lesions has successfully been carried out by High Resolution Melting Curve analysis (HRM) (74).

This system relies on the fact that the melting properties of doublestranded (ds) DNA amplicons differ in relation to sequence, GC-content and length.
When a PCR amplicon is melted in the presence of a dsDNA-binding fluorescent dye, loss of fluorescence can be measured and a characteristic melt curve for each sequence can be analysed by plotting the fluorescence intensity against the melting temperature.

Genome editing was analysed for two Zinc Finger Nucleases. B276 ZFN binds a 26 basepair stretch in *tmtopsb* exon 1 (position 276-302) and was injected at an amount of 10pg of each ZFN per injection volume. Genomic DNA for analysis was extracted at 2dpf. B282 ZFN binds 6bp further downstream in the same exon. It was injected at 60 pg each/ injection volume and here DNA extracted from 7 embryos fixed 2 dpf was used as PCR template. A plasmid construct encoding the *tmtopsb* target site with a 30 bp deletion served as control. For each sample two biological replicates with a template concentrations of 10 ng and 20 ng total were performed.

In figure 3.5 two plots are shown for each ZFN pair. For aligned melt curves the percentage of fluorescence is plotted against the temperature. At 100% fluorescence all DNA amplicons are present in their doublestranded from. With increasing temperature DNA melting occurs and results in a release of the fluoresecent dye and decrease in fluorescence. In the difference plot the curves are plotted against a reference, here the wildtype *tmtopsb* fragment.
In both plots a difference in melting curves between injected animals and even more pronounced between wildtype and insertion construct becomes apparent for B282 ZFN. The plots of the second ZFN, B276, on the contrary do not follow this pattern. Here the control was not included and the Zinc Finger pair was injected at a considerably lower concentration of only 10 pg/nl as compared to 60 pg/nl for B282 ZFN. This ZFN would also have to be injected in increasing concentrations, to test wether or not it is functional.

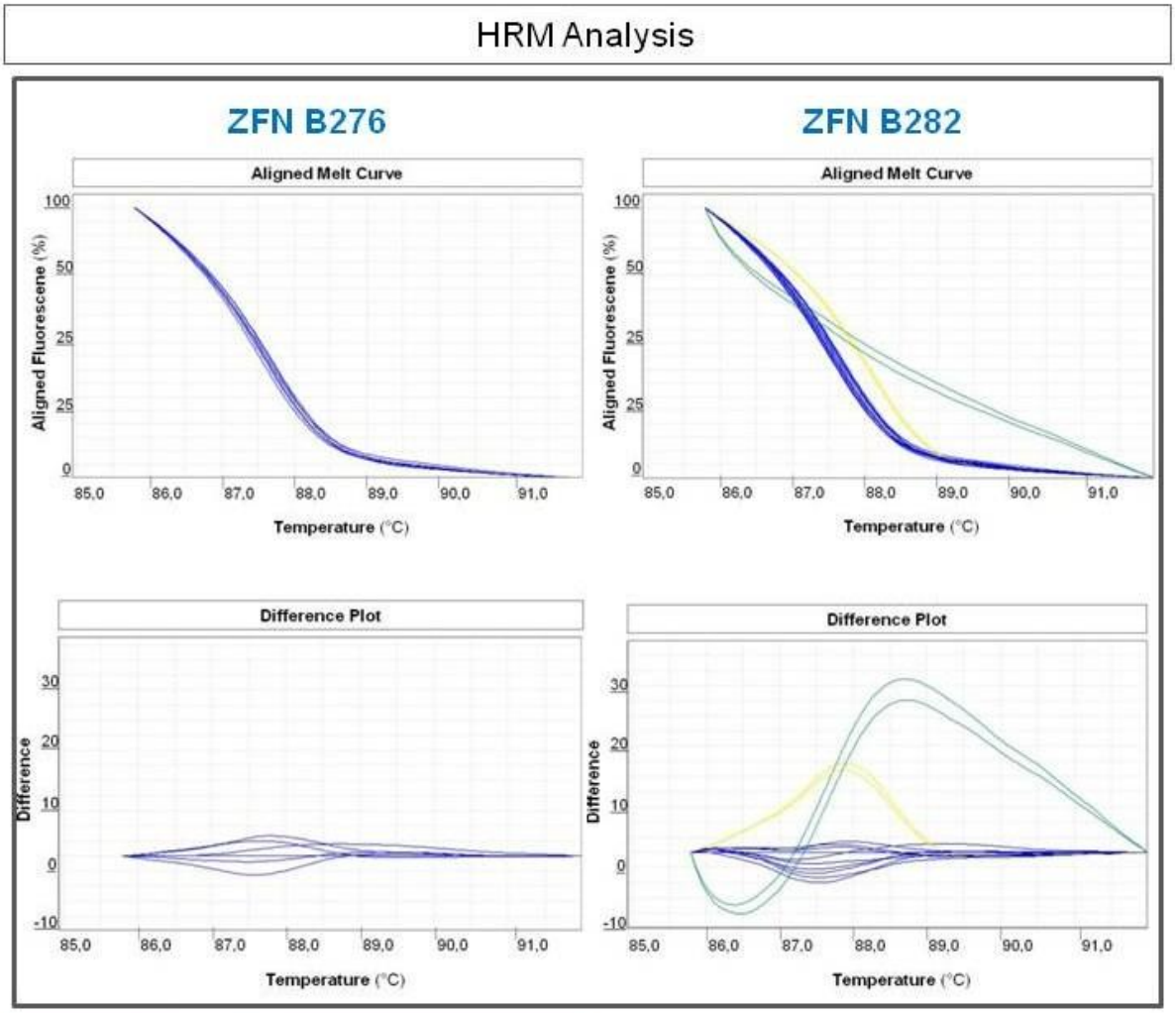

Ctrl	30 bp deletion
Injected	genomic DNA from 7 embryos injected with ZFN for tmtB at 60pg; fixed 2dpf
WT	Mix: genomic DNA from 10 embryos fixed 2dpf; Plasmid containing tmtB WT

Figure 3-5: High Resolution Melting Curve Analysis of genome editing in *tmtopsb*

Genome editing was analysed for two Zinc Finger Nucleases B276 ZFN and B282 ZFN. Both target *tmtopsb* exon 1. A plasmid construct encoding the *tmtopsb* target site with a 30 bp deletion served as control. For each sample two biological replicates with template concentrations of 10 ng and 20 ng total were performed.

For B 276 ZFN no difference in melting properties can be detected between the wildtype and genomic DNA of injected embryos.

On the right hand the curves for B282 ZFN are shown. In the aligned melt curves as well as a difference plot, each with the wildtype samples as reference, a clear variation between the curves can be observed. The green curve represents the control contruct and can clearly be distinguished from the wildtype. The curve obtained with genomic DNA of injected embryos is shown in yellow. Here also a clear difference to the wildtype becomes apparent. This suggests that genome editing at the target site occurred.

3.2.2 Summary

HRM analysis lead to the identification of a functional Zinc Finger Nuclease that targets a 5 bp spacer region at position 292 within the first exon of *tmtopsb* (Figure 3-5). In embryos injected with this ZFN genome editing must have occurred and sequencing analysis will have to be performed to determine the character of the mutation.

TMT-OpsinB is a very interesting candidate for functional studies on knock-out mutants since it is expressed in the amacrine cells of the eye and the presumptive annular ligament (27). In fish lacking this MTO a phenotype should become apparent, that will help to gain some insight into the role of TMT-OpsinB in eye development and morphology.

Targeted gene knock-outs of individual members of the multiple tissue opsin family make it possible to analyse which cellular functions are dependent on the opsin and in what way they are affected. Another question would be wether the different paralogoues of the four opsin classes are able to complement each others function and wether the silencing of one opsin affects the gene expression of its paralogue.
To address these questions mutant lines will have to be established and phenotypic and behavioural analysis can be performed to determine functional implications. Besides that whole mount *in situ* hybridization can be employed to assess changes in expression patterns of MTO homologues in fish where one opsin gene has been silenced.
To this date no published data exist on Zinc Finger mediated gene knock-out in Medaka. The data presented above show that this technology can successfully be employed in the teleost species and offers a new tool in reverse genetics in *Oryzias latipes*.

3.3 Expression analysis of Multiple Tissue Opsins in *Danio rerio*

Finally, I wanted to assess the expression patterns of the Multiple Tissue Opsins in Zebrafish larvae. After identifying a member of these opsins, Moutsaki et al. claimed that it was expressed in diverse tissues throughout the whole body (29). However this was called into question by whole mount *in situ* analysis where expression could only be detected in distinct areas of the brain at presumptive neurosecretory sites (30).

Also the novel TMT-Opsins identified by Stephan Kirchmaier showed a confinement to regions o the nervous system in their expression (27). All novel opsins had been cloned by Stephan Kirchmaier or Ruth Fischer and DIG- or Fluorescein-labeled RNA probes were synthesized as described above.

By looking again at the different expression patterns of the Zebrafish TMT-Opsins I wanted to address the following questions. Given that MTOs act as light sensors, it would be interesting to see if the absence of light during larval development changes the expression pattern of these photoreceptors. On the other hand I wanted to assess whether the expression domains overlap between the different MTO family members. Localisation of different opsins at the same distinct areas of the brain or strong differences in the expression patterns might hint towards functional implications. In addition to that I performed double stainings with different Fluorescein labeled markers to determine the identity of the TMT-Opsin expressing cells. In the following I will present the results obtained from *in situ* hybridization.

For *enc* and *tmtopsc2* no stainings could be detected. Here due to an unknow error in the procedure or faulty probes all samples for these genes only showed a very high background or no staining at all. Besides that it is possible that these genes are expressed only at certain time points during the day or at later stages of development, so I could not have detected them in the samples that I analysed.

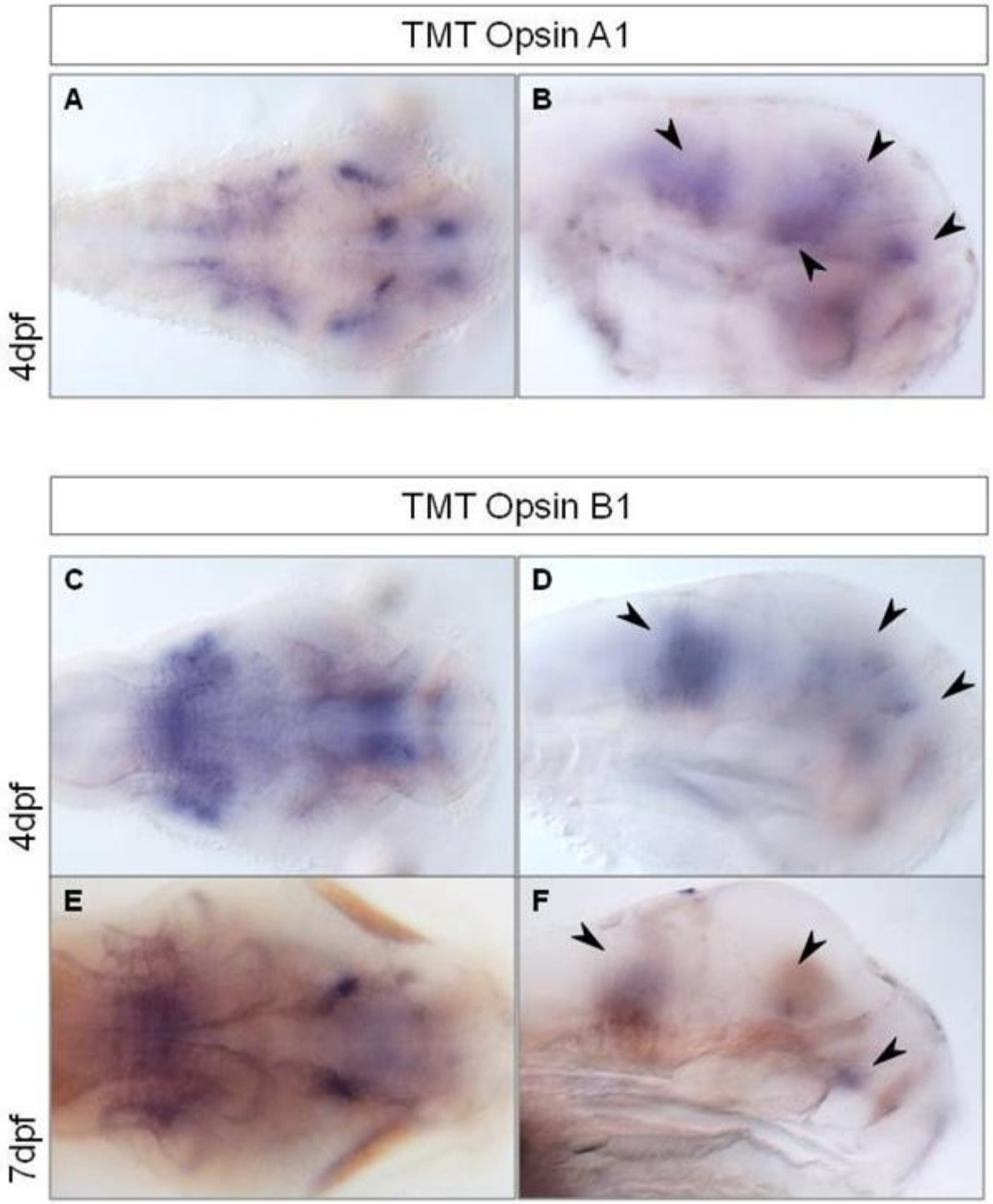

Figure 3-6: Brain expression of Teleost Multiple Tissue Opsins A1 and B1

Here the expression pattern of TMT-OpsinA1(A,B) and TMT-OpsinB1 (C-F) in larvae fixed 4 dpf and 7 dpf (for *tmtopsb1*) is shown. Both opsins are present in symmetric domains in the midbrain and in the hindbrain. These do not seem to change during larval development as shown for *tmtopsb1*. Here the staining at 7 dpf (E,F) is a little weaker compared to the younger stage. The fish are shown with the anterior to the left in a dorsal view on the left panel, and a lateral view on the right.

3.3.1 Expression of TMT Opsins at distinct nervous system domains

Zebrafish larvae fixed at 4 dpf and 7 dpf were analysed using Whole Mount *in situ* hybridization. After collecting the eggs, the batches were split and either incubated under normal light conditions or under constant darkness. For all the analysed Teleost Multiple Tissue Opsins an expression in distinct brain domains could be observed.

Except for TMT-B2, I could not detect a change in the pattern of the stainings when comparing different stages of development.

However it became apparent that generally the expression domains partly overlapp between different TMT-Opsins (Figure 3.6)

Deep brain photoreceptors have been demonstrated before in the hypothalamus and the pineal gland (16, 27, 30). Also now expression of TMT-OpsinA1 and the TMT-OpsinB family could be observed in symmetric domains within the diencephalon at the level of the habenulae and within the hypothalamus. The opsins were also present in the the midbrain and in the hindbrain in a relatively broad domain adjacent to the otic vesicles. For both *tmtopsa1* and *tmtopsb1* the expression pattern did not change during larval development and also the absence of light did not show an effect on the expression domains.

3.3.2 Partly overlapping brain expression domains between VA and MT Opsin families

In 2000 Philp et al. found a novel opsin family to be expressed in the diencephalon as well as in the inner retina (75). This Vertebrate Ancient (VA) Opsin was first found in the Atlantic Salmon and later on its homologue and an alternatively spliced isoform, the Vertebrate ancient long (VAL) opsin. was found in Zebrafish (15). Due to a duplication event there are two paralogues of the VAL-Opsin gene, i.e. *valopa* and *valopb* that show differential expression in the fish brain and the inner retina (6). As another family of non-visual photoreceptors also VAL-Opsins have been discussed as candidates for mediating photoperiod-dependent physiological events, such as the light-induced changes in body colour in Zebrafish (6, 69).

Since VAL-Opsins have been shown to be expressed in distinct areas of the diencephalon, I wanted to compare this pattern with the expression of TMT-Opsins.

An overview over VAL-Opsin expression in the brain is shown in figure 3.7. (probe against *valopb* mRNA: courtesy of Daisuke Kojima).

VAL-OpsinA can be detected in the habenulae, the midbrain and in a large domain in the hindbrain. This expression pattern strongly resembles that of the TMT-Opsins A1 and B1. VAL-OpsinB also is present in some cell clusters in the diencephalon and in two patches within the hindbrain, similar to TMT-OpsinB2.

Double *in situs* for VAL-OpsinA and TMT-OpsinA1 and VAL-OpsinB and TMT-OpsinB2 were performed. For the expression in the brain, some overlap could be observed. *tmtopsb2* and *valopb* are both expressed in two patches within the hindbrain.

A double *in situ* with a DIG-labeled probe for the VAL-Opsin and a fluorescein-labeled probe for the MTO showed that these cell clusters overlap only in part. The VAL-Opsin positive cells are situated in a layer above the *tmtospb2* expressing ones (Figure 3.8.)

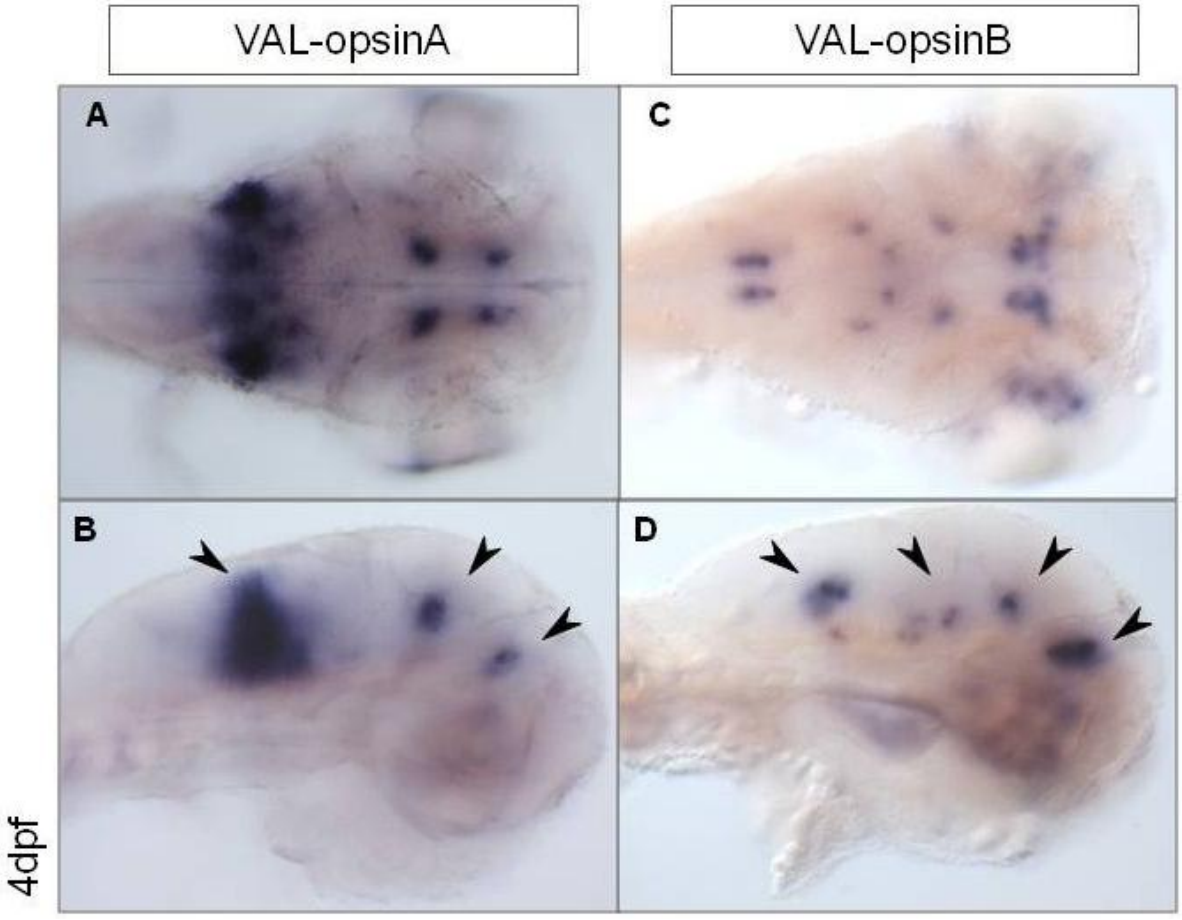

Figure 3-7: Expression of VAL-Opsin genes

Here an overview over the expression of VAL-OpsinB and VAL-OpsinA in 4-day old larvae is shown. VAL-OpsinA can be detected in the midbrain and hindbrain, VAL-OpsinB in the midbrain, among others in a cluster identified as the habunular nuclei by the authors (6) and in two symmetric patches within the hindbrain. When compared to MTO expression in the brain, an overlap in expression domains becomes apparent. Larvae are shown with the anterior to the right from a dorsal view on the top (A,C) and a lateral view on the bottom (B,D). (Ocular expression is not shown here.)

For TMT-OpsinA1 and VAL-OpsinA expression in two disctinct cell clusters in the midbrain cleary overlapped (Figure 3.9). Here the probe for TMT-OpsinA1 was labeled with digoxigenin and the VAL-Opsin probe was fluorescein-labeled.
For the other opsins or expression domains, except for the eyes, no clear overlap could be detected due to very high background of the staining or failure of the *in situ* due to an unknown error during the procedure.

However the comparison between the expression patterns of VAL-Opsins and MTOs shows that there are several photosensitive domains within the midbrain and hindbrain that appear to be relatively abundant and harbor deep brain photoreceptors that express different sets of non-visual opsins.

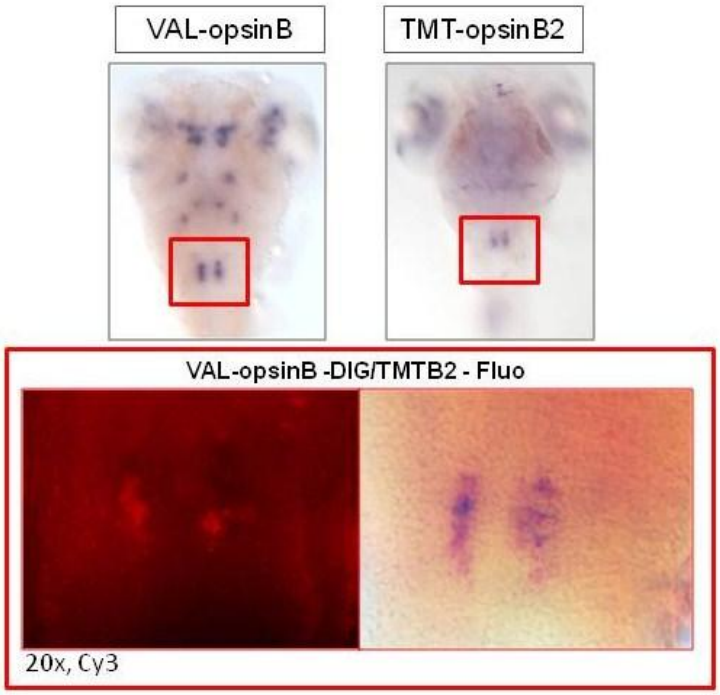

Figure 3-8:-Overlapping expression between *valopb* and *tmtopsb2*

Double *in situ* hybridization with a DIG-labeled probe against TMT-OpsinB2 mRNA and a fluorescein-labeled probe against VAL-OpsinB. In the upper panel an overview over both expression patterns is shown in 4 day old fish with the anterior to the top from a dorsal view. The lower panel shows the result from a double *in situ* with a fluorescent view on the left and a light transmission image on the right. Here a clear overlap in the expression domain can be observed, however the VAL-OpsinB positive cells cluster in a cell layer located further dorsal than the MTO-expressing cells.

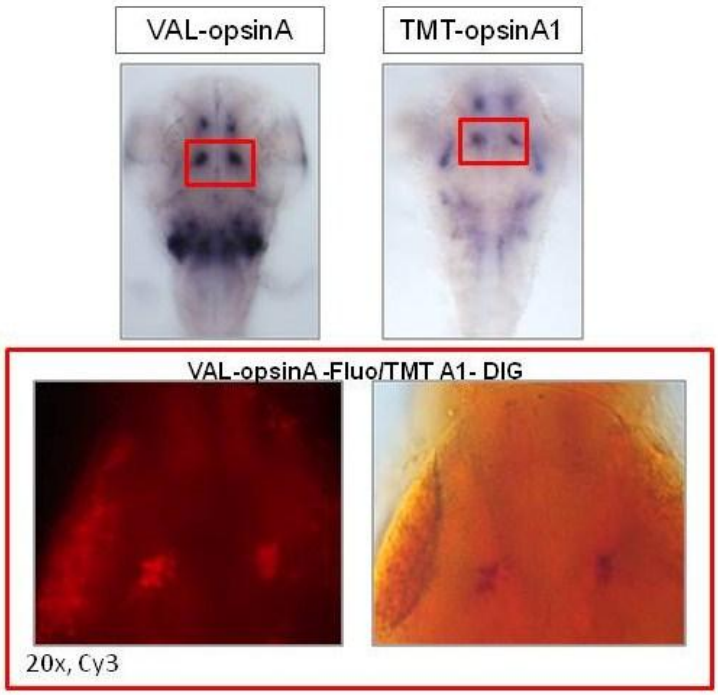

Figure 3-9:-Overlapping expression between *valopa* and *tmtopsa1*

Here a double *in situ* with a DIG.labeled probe agaist TMT A1 and a fluorescein-labeled probe against VAL-OpsinA mRNA shows a common expression domain in the midbrain for the two non-visual photoreceptors. In the upper panel an overview of larvae fixed at 4dpf shows this symmetric staining (red box). The fish are arranged with the anterior to the top. All images are taken from a dorsal view. The bottom panel shows a 20x amplification of the marked region in the double stained samples, with a fluorescent image of VAL-OpsinA on the left.

3.3.3 Expression of *tmtopsB2* in Zebrafish larvae

The expression of all TMT-Opsins that were analysed was confined to the central nervous system, except for TMT-OpsinB2 that is expressed in the eyes and in two stripes at the swim bladder, ventrally of the spinal chord (Figure 3.10). Besides that B2 is strongly expressed in the pineal and in two symmetric cell clusters in the hindbrain. At 4dpf an expression at the midbrain-hindbrain boundary can be observed. This was not seen at the later stage. Interestingly *tmtopsb2* is the only of the analysed TMT-Opsins to be expressed in the pineal and the expression between the two homologues TMT-OpsinB1 and B2 differs greatly.

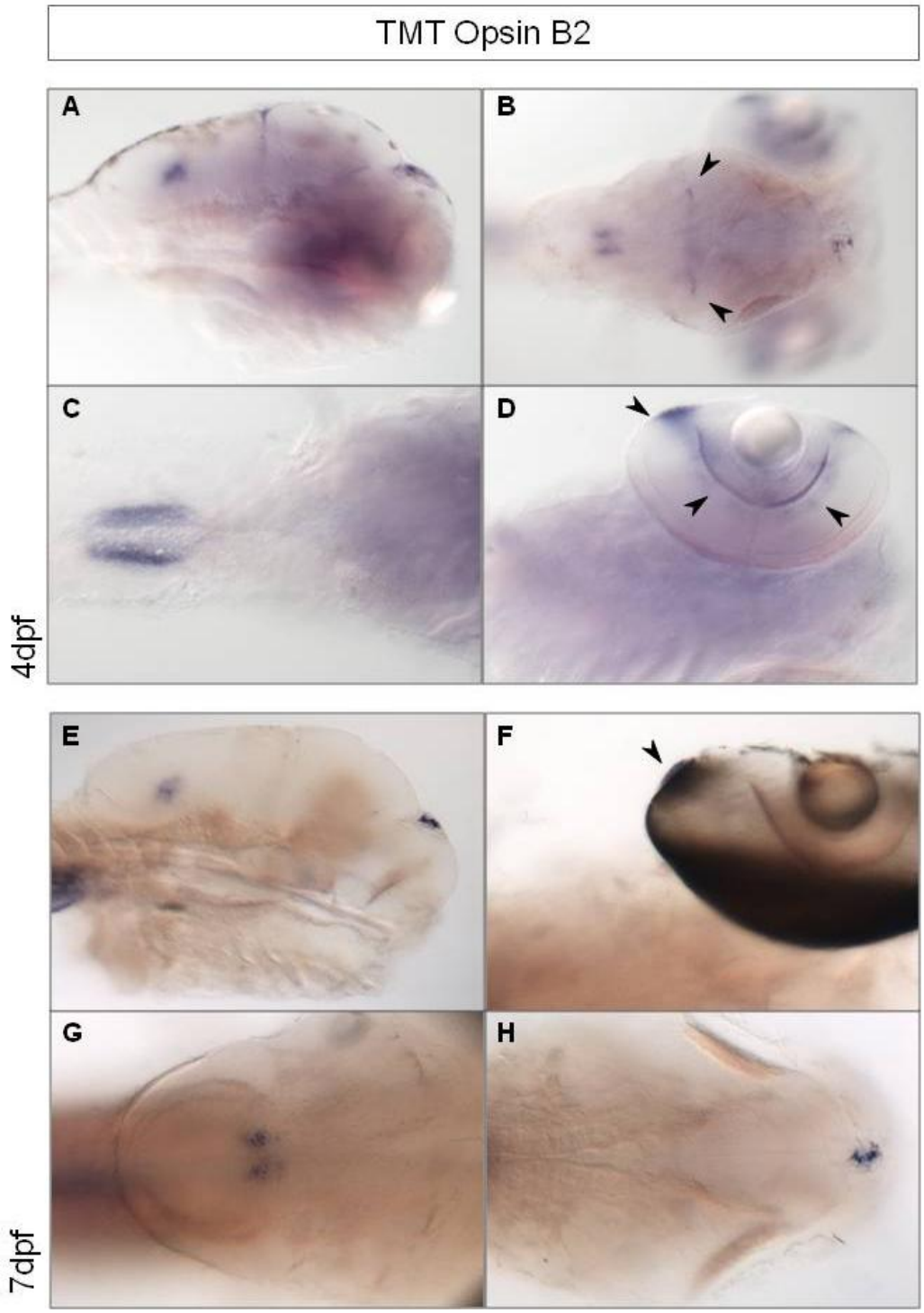

Figure 3-10:Expression pattern of TMT-Opsin B2

Here the expression of TMT Opsin B2 was analysed via whole mount *in situ* hybridisation in 4 day old (A-D) and 7 day old (E-H) larvae. At both time points expression can be observed in the pineal and in two symmetric domains in the hindbrain. At 4dpf a staining at the midbrain-hindbrain boundary is clearly visible (B;black arrows). This seems to be lost at the later stage. Also the expression in the eyes changes during development. At 4dpf the gene is expressed at the iridocorneal angle and a subset of inner retinal cells. At 7dpf only expression at the iridocorneal angle can be observed. Besides that a staining appears in two stripes above the swimbladder (C; here only shown for 4dpf). All larvae are shown with the anterior facing to the right (A,E –lateral view; B,C,D,F,G,H –dorsal view)

Comparison with Medaka *tmtopsb* showed that the pattern is conserved between the two teleost species. Here the TMT-Opsin can be detected in the hindbrain, the eyes, the pineal and within the diencephalon (27).

Also for B2 no obvious difference could be distinguished by microscopic observation between larvae that developed under normal light conditions and those that were incubated in complete darkness.
TMT-OpsinB2 is the only Mulitple Tissue Ospsin that is present outside of the brain. It can be detected in two stripes at the dorsal side of the swimbladder (Figure 3.10, C). By regulating the volume of the swim bladder the fish can change their vertical position in the water column (76-77). It has been shown that this vertical positioning underlies a diurnal rhythm among other factors (76). It is possible that here TMT-OpsinB2 is involved in controlling the swimbladder volume in correlation to light intensity.

3.3.3 Eye-specific expression of *tmtb2*

As described above TMT B2 was detected in distinct cell layers of the Zebrafish eye. At 4 dpf a staining became visible in the amacrine cell layer of the eye. Besides that a stanining at the iridocorneal angle, forming a semi-circle around the lens, could be observed (Figure 3.10, 3.11). This second domain remained visible also at later stages and even in adult eyes expression of *tmtopsb2* at a circular structure in the anterior segment of the eye was detected (Figure 3.12). In larvae, where pigmentation had not been inhibited by PTU it became apparent that the opsins is expressed in cells located within the cornea above the retinal pigmented epithelium (Figure 3.11).
To determine the identity of these cells double stainings with two markers were performed. On the one hand CCNDI (cycline dependent kinase inhibitor 1c or p57), specifically marking proliferating cells, was used. In the eye cell proliferation occurs at the ciliary marginal zone, a stem cell niche at the rim of the retina (78).
On the other hand a marker for the annular ligament, a connective tissue within the anterior segment of the eye, was used as a reference to determine the tissue in which *tmtopsb2* is active.

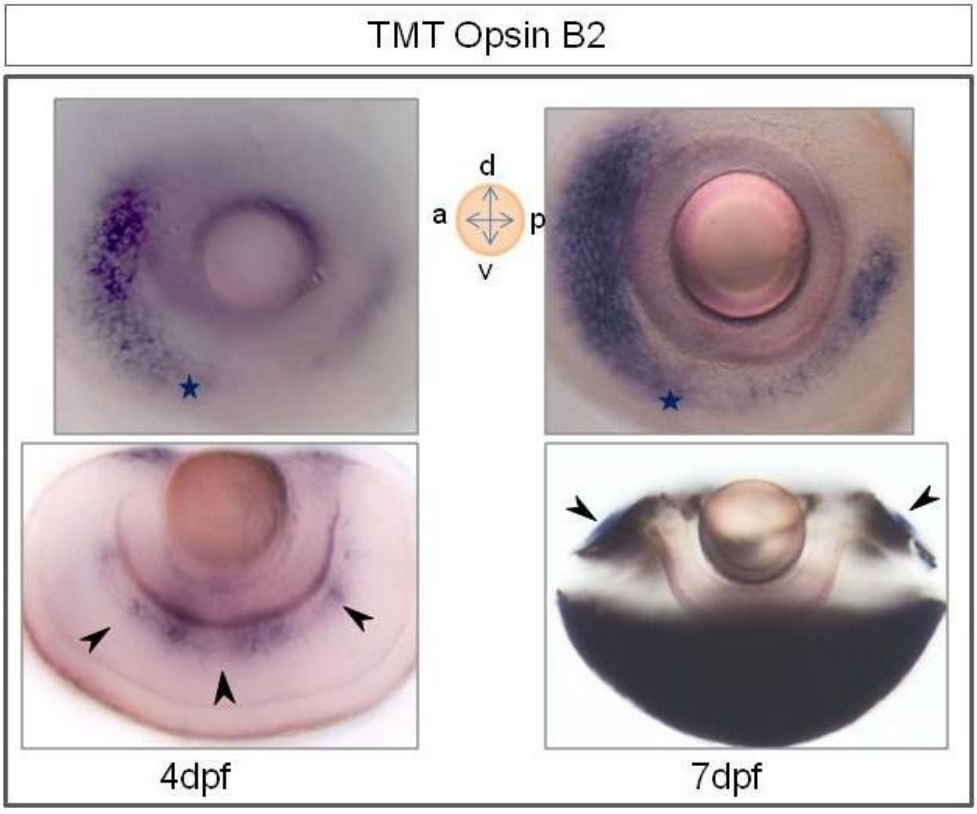

Figure 3-11: Ocular expression of *tmtopsb2*

TMT-OpsinB2 is found in two distinct tissues of the eye. A semi-circular cell cluster at the iridocorneal angle is stained at both 4 dpf and 7 dpf. At the later stage this staining seems more pronounced and from the lateral view of a pigmented eye it becomes apparent that these cells are located above the pigmented layer. At 4 dpf expression can also be detected in the inner retina in a subset of amacrine cells, as shown in the lateral view. The asteriks in the upper images marks the location of the Schlemm's canal for better orientation. (a – anterior, d – dorsal, p – posterior, v – ventral)

The annular ligament can be labeled with a probe against Scinderin-like a (Scinla) mRNA, a homologue of the actin-binding protein gelsolin (79). Scinla is expressed at the iridocorneal angle, in a specialized tissue of the cornea (80). Stainings with these two markers showed that *tmopstb2* is expressed in the annular ligament of the eye (Figure 3-13).

In teleost eyes focusing of incoming light happens by moving the large spherical lens vertically within the optic cup (81). But light scattering and refraction also occurs in the cornea, mediated by corneal crystallins (82).

The cornea is part of the ocular anterior segment which is also comprised of iris, lens, ciliary body and the annular ligament at the iridocorneal angle (83).

The annular ligament has be ascribed three functions, the regulation of the intraocular pressure and corneal curvature for focusing incoming light as well as structural stabilisation of the anterior eye (84).

The presence of a photopigment at this structure implements a dependance of these functions from light stimuli. It suggests that TMT-OpsinB2 is involved in mediating corneal curvature and transparency dependent on differing light conditions.

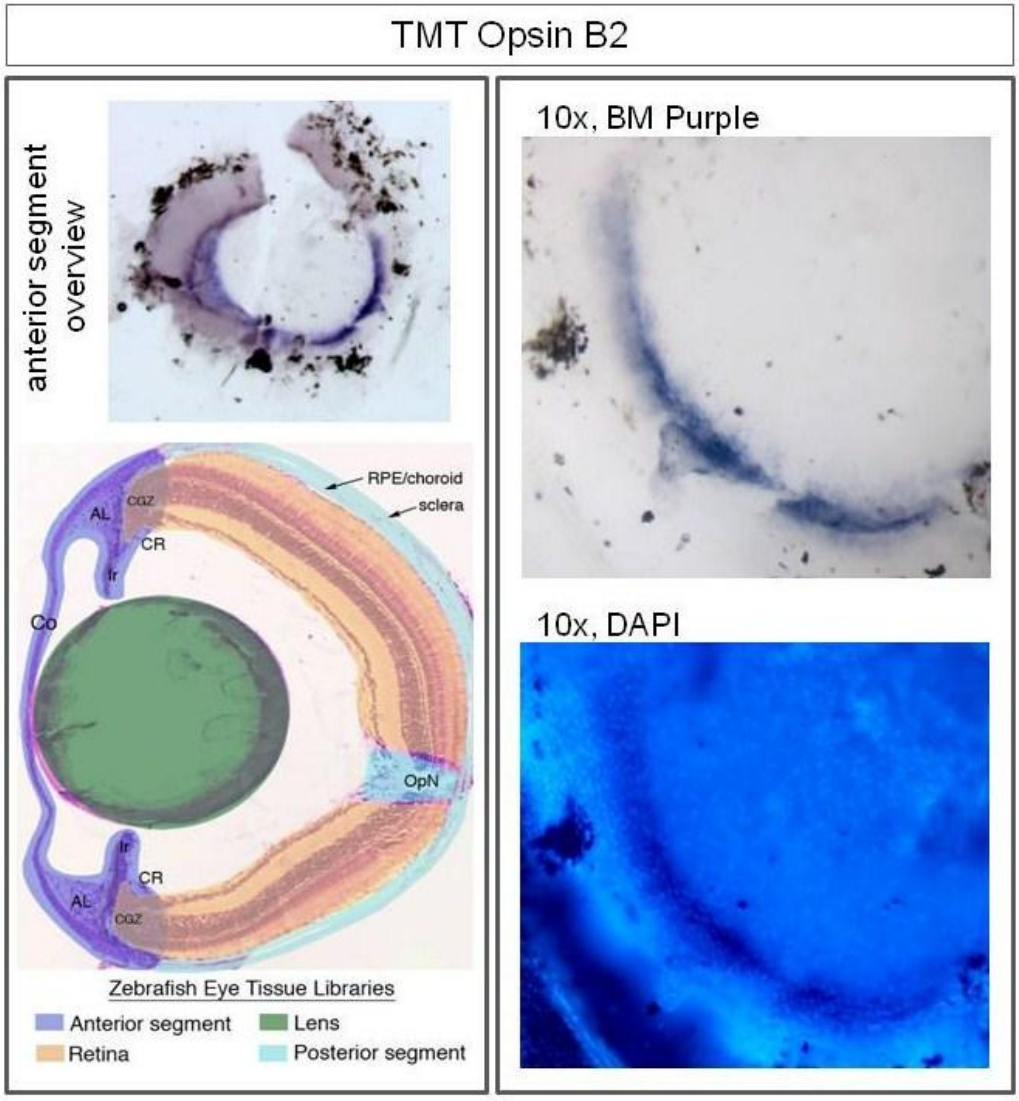

Figure 3-12: Expression of *tmtopsb2* in the adult anterior segment

Adult eyes were fixed and the dissected anterior segment was used for *in situ* hybridization. Also in the adult tissue the ring-like staining of *tmtopsb2* expressing cells could be observed. On the schematic depiction of the eye the anatomy of the anterior segment can be seen (Figure from (85)). A DAPI staining on the left shows that the observed structure is indeed cellular. (AL- annular ligament, CR – ciliary region, CGZ – retinal margin, Co –Cornea, Ir –iris, OpN – optic nerve, RPE –retinal pigmented epithelium)

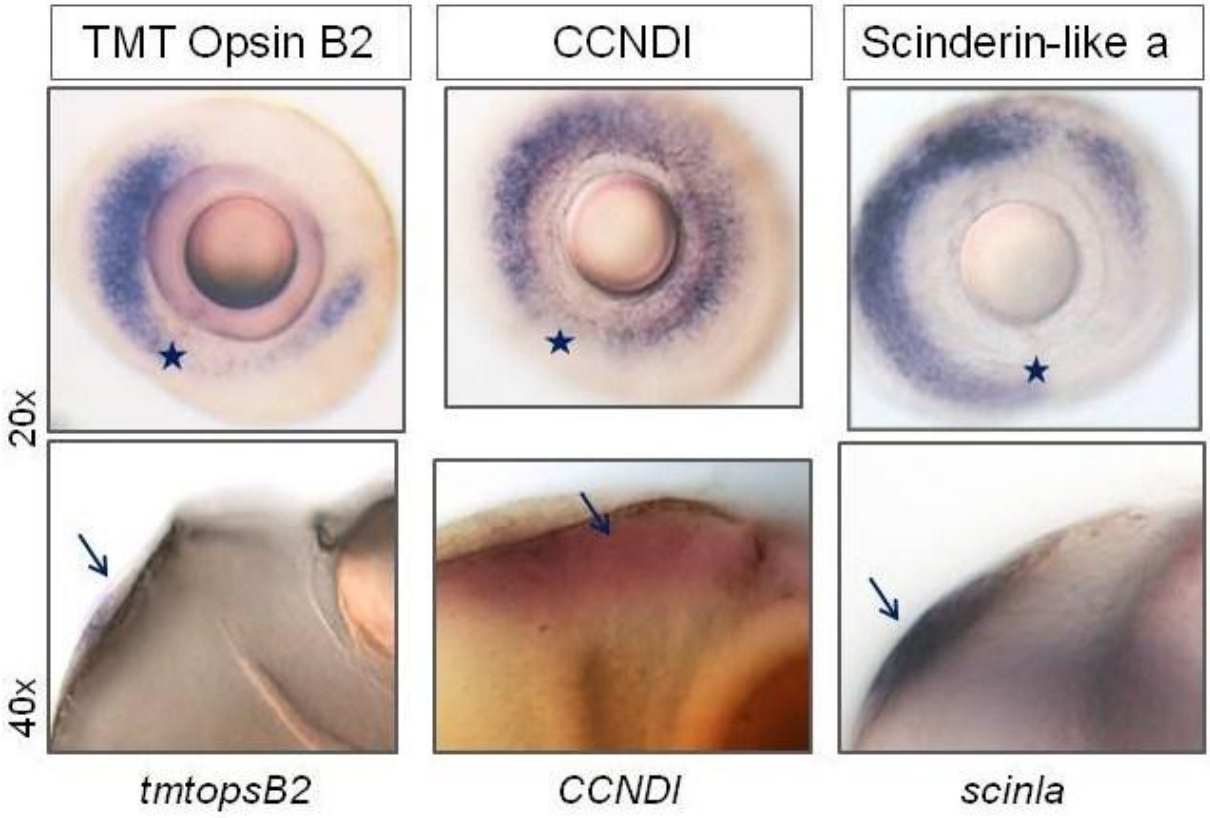

Figure 3-13: Determining the cell identity of *tmtopsb2* expressing cells

Here a comparison of TMT B2 positive cell with the ciliary marginal zone (*CCNDI*) and the annular ligament (*scinla*) is shown in a 20x amplification in the upper panel and 40x at the bottom. For this *in situ* 7 day old larvae of the mitfa strain were fixed and treated with PTU to inhibit pigmentation. In the 40x image CCDNI is stained with Fast Red. The asteriks marks the Schlemm's canal for orientation. The arrows indicate that the MTO is clearly expressed in the same cell layer as the annular ligament marker. This layer is situated above the retinal margin, at the iridocorneal angle.

3.3.4 VAL-Opsins and TMT-OpsinB2 show partly overlapping expression in the eye

In the next step I compared the ocular expression of the two non-visual opsin families, the VAL-Opsins and TMT-OpsinB2 in larvae fixed 4 dpf. Besides that I performed double stainings with the multiple tissue opsin and the respective VAL-Opsins. VAL-OpsinA is present only in the anterior segment of the eye, VAL-OpsinB can be found in a subset of amacrine cells in the inner retina. TMT-Opsin B2 can be detected in both (Figure 3.11, 3.14).

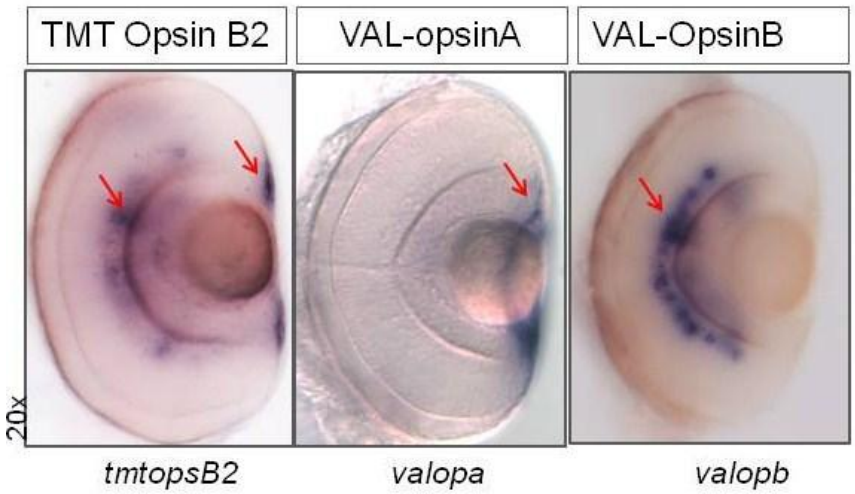

Figure 3-14: Ocular expression of non-visual opsins

While *tmtopsb2* is detected in both the amacirne cells and the anterior segment, this differs for the two VAL-Opsins. *valopa* expression is found in the anterior segment, its paralogue *valopb* shows staining in the amacrine cells. The eyes of 4 day old larvae are shown from the side with the optic nerve towards the left.

Double in situs showed that on the one hand the expression domains differ. VAL-OpsinA is present in the iris (6). The cell layer is closer to the lens and does not overlap with the region of the annular ligament. On the other hand, in the inner retina both VAL-OpsinB and TMT-OpsinB2 are detected in the amacrine cells (Figure 3-14).

In the inner retina several types of intermediate neurons are involved in signal transmission. The amacrine cells are involved in transmitting the input from rod and cone photoreceptors via the bipolar and horizontal cells to the retinal ganglion cells, that form the connection between the eyes and the brain via the optic nerve (86). Opsin expression in the inner retina has been well described. Intrinsically photoreceptive Retinal Ganglion Cells (ipRGCs) express melanopsin, the photopigment involved in circardian photoentrainment, on their surface (10, 87). Also VA-Opsin is present in the inner retina (88). The role of these photopigments is not entirely clear, however they are suggested to play a part in the intrinsic photoentrainment of the retina and functions such regulation of light-dependent pupillary reflexes (89).

Here double *in situ* hybridisation showed, that both analysed non-visual opsins are expressed in subsets of amacrine cells.

These subsets appear to be specific for both photopigments, however they overlap to some extent. Interestingly VAL-OpsinB expression in the amacrines could also be deteceted at 7 dpf (data not shown) while TMT-OpsinB2 seems to be restricted to the annular ligament at the later stage.

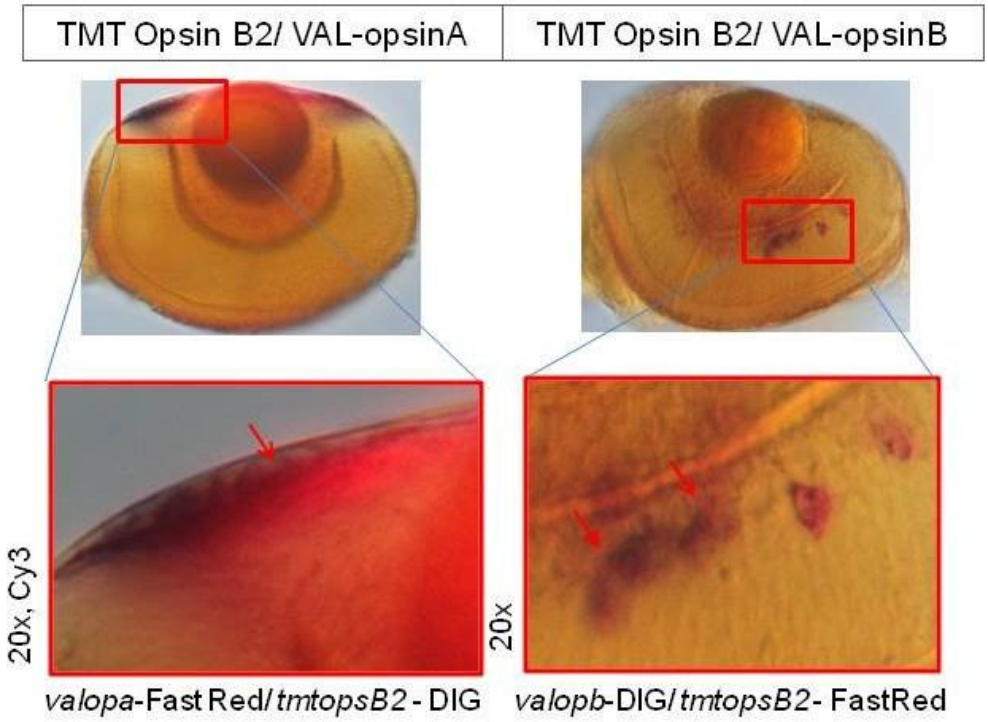

Figure 3-15: Differential expression of VAL-Opsins and TMT-OpsinB2

While in the iris no overlap between the two non-visual photoreceptors could be observed, also shown in an overlayed image with VAL-OpsinA stained with Fast Red and TMTB2 with BM Purple, co-expression of *valopb* and *tmtopsb2* in some sets of amacrine cells is shown on the right. The eyes of 4 day old larvae are shown with the anterior segment towards the top from a lateral view.

3.3.5 Summary

In situ hybridization and visualization of Mulitple Tissue Opsin expressing cells has confirmed the confinement of their expression domains to the central nervous system.

These domains are spread across the diencephalon, mesencephalon and rhombencephalon and the high abundance of photoreceptive sites within these structures suggests that the brain is directly involved in the non-visual sensory process.

The role of deep brain photoreceptors in the entrainment of the circadian clock and twilight and irradiance detection has long been discussed and a number of photopigments have been identified in tissues of the nervous system (90).VAL-Opsins for example have been correlated with the regulation of light induced changes in body colour (69) and pineal opsins are involved in photic regulation of melatonin synthesis and circadian responses (90). Extra-retinal photoreceptors have also been implemented in light-induced locomotor activity (70).

The role of TMT-Opsins in the non-visual sensory process however is still unclear. The results presented above demonstrate though, that they belong to the group of deep brain photoreceptors, that cluster together in photosensitive centers throughout large portions of the central nervous system. As far as these centers are concerned, the expression patterns seem to remain conserved in the larvae independently of a light input. However, it is difficult to draw a conclusion on the expression levels from *in situ* analyses and it might be necessary to employ more sensitive methods, such as quantitative real-time PCR.

For retinal rod and cone opsins for example this showed that the photopigment renewal is dependent on light stimuli and a deprivation of light leads to a change in gene expression (91). It would be interesting to analyze on which factors the turn-over of MTOs depends and to what extent light intensities and wavelengths account for the levels of opsin expression.

Analysing the light sensitivity of the pigments and correlation of exposure to light of different intensities to gene expression will help to elucidate the function of the individual MTO family members.

Despite previous evidence (29) only TMT-OpsinB2 could be detected outside of the brain in Zebrafish as well as in Medaka larvae. Its presence in the annular ligament of the eye even in adult Zebrafish suggests that this opsin is indirectly involved in the visual process, by regulation of corneal curvature and transparency dependent on changing light conditions. Expression in the inner retina suggests a function of *tmtopsb2* in circadian entrainment (92), however there is a great diversity of amacrine sub-types, whose function is not entirely clear (93). The Opsin cannot be detected in the amacrine cells at later stages, which could imply a function in developmental processes. On the other hand its presence in the inner retina cannot be excluded from *in situ* results, since it might still be expressed, only at low RNA levels. Immunohistological analysis with an antibody against the protein could be used to futher investigate this.

Seeing that TMT-OpsinB2 is also expressed in the adult tissue it would be interesting to analyse this also for the VAL-Opsins as well as for *tmtopsb* in Medaka. Also *encephalopsin* has been detected in the eyes of adult mice (24).

It would be interesting to see wether this expression profile is conserved also in lower vertebrates and in which ocular tissue this MTO is detected.

4 Conclusion

The creation of reporter lines and knock-out mutants is an essential step in the process of unravelling the biological function of Multiple Tissue Opsins. In the course of my project I took two approaches to advance this process. For Zebrafish I wanted to establish reporter lines via BAC mediated transgenesi to label and later on specifically ablate Multiple Tissue Opsin – expressing cells. In Medaka I tested specifically designed Zinc Finger Nucleases to target *tmt-opsin* genes and create knock-out mutants.

For the generation of transgenic Zebrafish reporter lines I adapted different protocols to establish a functional recombineering pipeline for BAC modifications where problems, such as the recombination of bacterial genomic DNA with the *rpsLneo* homology cassette and inactivation of streptomycine sensitivity, essential for the recombineering process, were circumvented. I was able to inject two BAC constructs into Zebrafish embryos and detected heart specific expression of a transgenesis marker, i.e. *mcherry* expressed under the cardiac myosin light chain promoter cmlc2, at 2dpf. However I was not able to demonstrate a labelling of *tmtopsin* expressing cells.
In Medaka I identified a functional Zinc Finger Nuclease for targeted gene knock-out of *tmtopsb*. I showed that the High Resolution Melting Curve analysis is a method sensitive enough to detect ZFN-induced lesions and can be used as a relatively quick read-out assay to identify genomic mutations in injected larvae.

Lastly I was able to determine the expression patterns of several TMT-Opsins in the brain and eyes of Zebrafish. Comparison of TMT-OpsinA1, B1 and B2 to another class of non-visual opsins, the VAL-Opsins, showed that the novel deep brain photoreceptors are present in discrete regions of the brain outside of the known photoreceptive areas. This abundance of directly photoreceptive sites in the central nervous system implies a far more pronounced role of the brain as sensory organ as previously assumed. For *tmtopsb2* I determined the anatomical position at which this opsin is present in the eye of larval and adult Zebrafish, namely the annular ligament. This leads me to the assumption that TMT-OpsinB2 and its Medaka homologue TMT-OpsinB are indirectly involved in the visual process by regulating the corneal structure and transparency in accordance to changing light conditions. .

5 References

1. Hut RA, Beersma DG. Evolution of time-keeping mechanisms: early emergence and adaptation to photoperiod. Philos Trans R Soc Lond B Biol Sci. 2011;366(1574):2141-54. PMCID: 3130368.

2. Foster RG, Soni BG. Extraretinal photoreceptors and their regulation of temporal physiology. Rev Reprod. 1998;3(3):145-50.

3. Philp AR, Bellingham J, Garcia-Fernandez J, Foster RG. A novel rod-like opsin isolated from the extra-retinal photoreceptors of teleost fish. FEBS Lett. 2000;468(2-3):181-8.

4. Shand JaF, R.G. The extra-retinal photoreceptors of non-mammalian vertebrates In: Archer SN, Djamgoz, M.B.A., Loew, E.R., Partridge, J.C. and Vallerga, S., Eds., editor. Adaptive Mechanisms in the Ecology of Vision Kluwer Academic Publishers; 1999. p. 197-222.

5. Archer SN. Light and photoreception: Visual pigments and photoreception. In: Archer SN, Djamgoz, M.B.A., Loew, E.R., Partridge, J.C. and Vallerga, S., Eds, editor. Adaptive Mechanisms in the Ecology of Vision Kluwer Academic Publishers1999. p. 25-41.

6. Kojima D, Torii M, Fukada Y, Dowling JE. Differential expression of duplicated VAL-opsin genes in the developing zebrafish. J Neurochem. 2008;104(5):1364-71. PMCID: 2702163.

7. Mano H, Kojima D, Fukada Y. Exo-rhodopsin: a novel rhodopsin expressed in the zebrafish pineal gland. Brain Res Mol Brain Res. 1999;73(1-2):110-8.

8. Okano T, Takanaka Y, Nakamura A, Hirunagi K, Adachi A, Ebihara S, et al. Immunocytochemical identification of pinopsin in pineal glands of chicken and pigeon. Brain Res Mol Brain Res. 1997;50(1-2):190-6.

9. Okano T, Yoshizawa T, Fukada Y. Pinopsin is a chicken pineal photoreceptive molecule. Nature. 1994;372(6501):94-7.

10. Rollag MD, Berson DM, Provencio I. Melanopsin, ganglion-cell photoreceptors, and mammalian photoentrainment. J Biol Rhythms. 2003;18(3):227-34.

11. Vigh B, Manzano e Silva MJ, Frank CL, Vincze C, Czirok SJ, Szabo A, et al. The system of cerebrospinal fluid-contacting neurons. Its supposed role in the nonsynaptic signal transmission of the brain. Histol Histopathol. 2004;19(2):607-28.

12. Joly JS, Osorio J, Alunni A, Auger H, Kano S, Retaux S. Windows of the brain: towards a developmental biology of circumventricular and other neurohemal organs. Semin Cell Dev Biol. 2007;18(4):512-24.

13. Vigh-Teichmann I, Vigh B. The system of cerebrospinal fluid-contacting neurons. Arch Histol Jpn. 1983;46(4):427-68.

14. Fu Y, Zhong H, Wang MH, Luo DG, Liao HW, Maeda H, et al. Intrinsically photosensitive retinal ganglion cells detect light with a vitamin A-based photopigment, melanopsin. Proc Natl Acad Sci U S A. 2005;102(29):10339-44. PMCID: 1177370.

15. Kojima D, Mano H, Fukada Y. Vertebrate ancient-long opsin: a green-sensitive photoreceptive molecule present in zebrafish deep brain and retinal horizontal cells. J Neurosci. 2000;20(8):2845-51.

16. Vigh Bea. Nonvisual photoreceptors of the deep brain pineal organs and retina. Histology and Histopathology. 2002;17:555-90.

17. Fredriksson R, Schioth HB. The repertoire of G-protein-coupled receptors in fully sequenced genomes. Mol Pharmacol. 2005;67(5):1414-25.

18. Fredriksson R, Lagerstrom MC, Lundin LG, Schioth HB. The G-protein-coupled receptors in the human genome form five main families. Phylogenetic analysis, paralogon groups, and fingerprints. Mol Pharmacol. 2003;63(6):1256-72.

19. Terakita A. The opsins. Genome Biol. 2005;6(3):213. PMCID: 1088937.

20. Shichida Y, Matsuyama T. Evolution of opsins and phototransduction. Philos Trans R Soc Lond B Biol Sci. 2009;364(1531):2881-95. PMCID: 2781858.

21. Eakin RM. Morphology of invertebrate photoreceptors. Methods Enzymol. 1982;81:17-25.

22. Arendt D. Evolution of eyes and photoreceptor cell types. Int J Dev Biol. 2003;47(7-8):563-71.

23. Blackshaw S, Snyder SH. Encephalopsin: a novel mammalian extraretinal opsin discretely localized in the brain. J Neurosci. 1999;19(10):3681-90.

24. Tarttelin EE, Bellingham J, Bibb LC, Foster RG, Hankins MW, Gregory-Evans K, et al. Expression of opsin genes early in ocular development of humans and mice. Exp Eye Res. 2003;76(3):393-6.

25. Halford S, Freedman MS, Bellingham J, Inglis SL, Poopalasundaram S, Soni BG, et al. Characterization of a novel human opsin gene with wide tissue expression and identification of embedded and flanking genes on chromosome 1q43. Genomics. 2001;72(2):203-8.

26. Kasper G, Taudien S, Staub E, Mennerich D, Rieder M, Hinzmann B, et al. Different structural organization of the encephalopsin gene in man and mouse. Gene. 2002;295(1):27-32.

27. Kirchmaier S. Towards a molecular and functional characterisation of sensory-neurosecretory cells in Platynereis dumerilii and fish [Diplomarbeit]. Vienna: Universität Wien; 2009.

28. White JH, Chiano M, Wigglesworth M, Geske R, Riley J, White N, et al. Identification of a novel asthma susceptibility gene on chromosome 1qter and its functional evaluation. Hum Mol Genet. 2008;17(13):1890-903.

29. Moutsaki P, Whitmore D, Bellingham J, Sakamoto K, David-Gray ZK, Foster RG. Teleost multiple tissue (tmt) opsin: a candidate photopigment regulating the peripheral clocks of zebrafish? Brain Res Mol Brain Res. 2003;112(1-2):135-45.

30. Tessmar-Raible K, Raible F, Christodoulou F, Guy K, Rembold M, Hausen H, et al. Conserved sensory-neurosecretory cell types in annelid and fish forebrain: insights into hypothalamus evolution. Cell. 2007;129(7):1389-400.

31. Goodson JL, Thompson RR. Nonapeptide mechanisms of social cognition, behavior and species-specific social systems. Curr Opin Neurobiol. 2010;20(6):784-94.

32. Donaldson ZR, Young LJ. Oxytocin, vasopressin, and the neurogenetics of sociality. Science. 2008;322(5903):900-4.

33. Stenkamp RE, Teller DC, Palczewski K. Crystal structure of rhodopsin: a G-protein-coupled receptor. Chembiochem. 2002;3(10):963-7.

34. Terakita A, Yamashita T, Shichida Y. Highly conserved glutamic acid in the extracellular IV-V loop in rhodopsins acts as the counterion in retinochrome, a member of the rhodopsin family. Proc Natl Acad Sci U S A. 2000;97(26):14263-7. PMCID: 18906.

35. Terakita A, Koyanagi M, Tsukamoto H, Yamashita T, Miyata T, Shichida Y. Counterion displacement in the molecular evolution of the rhodopsin family. Nat Struct Mol Biol. 2004;11(3):284-9.

36. Palczewski K, Kumasaka T, Hori T, Behnke CA, Motoshima H, Fox BA, et al. Crystal structure of rhodopsin: A G protein-coupled receptor. Science. 2000;289(5480):739-45.

37. Karnik SS, Khorana HG. Assembly of functional rhodopsin requires a disulfide bond between cysteine residues 110 and 187. J Biol Chem. 1990;265(29):17520-4.

38. Flicek P, Amode MR, Barrell D, Beal K, Brent S, Chen Y, et al. Ensembl 2011. Nucleic Acids Res. 2011;39(Database issue):D800-6. PMCID: 3013672.

39. Sprague J, Bayraktaroglu L, Clements D, Conlin T, Fashena D, Frazer K, et al. The Zebrafish Information Network: the zebrafish model organism database. Nucleic Acids Res. 2006;34(Database issue):D581-5. PMCID: 1347449.

40. Signore IA, Guerrero N, Loosli F, Colombo A, Villalon A, Wittbrodt J, et al. Zebrafish and medaka: model organisms for a comparative developmental approach of brain asymmetry. Philos Trans R Soc Lond B Biol Sci. 2009;364(1519):991-1003. PMCID: 2666085.

41. Meyer A, Van de Peer Y. From 2R to 3R: evidence for a fish-specific genome duplication (FSGD). BioEssays. 2005;27(9):937-45.

42. Furutani-Seiki M, Wittbrodt J. Medaka and zebrafish, an evolutionary twin study. Mech Dev. 2004;121(7-8):629-37.

43. Lynch M, Conery JS. The evolutionary fate and consequences of duplicate genes. Science. 2000;290(5494):1151-5.

44. Lawrence C. The husbandry of zebrafish (Danio rerio): A review. Aquaculture. 2007;269(1-4):1-20.

45. Wittbrodt J, Shima A, Schartl M. Medaka--a model organism from the far East. Nat Rev Genet. 2002;3(1):53-64.

46. C.S. Koger SJT, and D.E. Hinton. Variations of Light and Temperature Regimes and Resulting Effects on Reproductive Parameters in Medaka (Oryzias latipes)1. Biology of reproduction. 1999.

47. Suster ML, Sumiyama K, Kawakami K. Transposon-mediated BAC transgenesis in zebrafish and mice. BMC Genomics. 2009;10:477. PMCID: 2768751.

48. Harshan Pisharath1, Jerry M. Rhee2,†, Michelle A. Swanson2, Steven D. Leach2,3, and, Michael J. Parsons2. Targeted ablation of beta cells in the embryonic zebrafish pancreas using E.coli nitroreductase. Mech Dev Author manuscript. 2007.

49. Springer B, Kidan YG, Prammananan T, Ellrott K, Bottger EC, Sander P. Mechanisms of streptomycin resistance: selection of mutations in the 16S rRNA gene conferring resistance. Antimicrob Agents Chemother. 2001;45(10):2877-84. PMCID: 90746.

50. Ejsmont RK, Sarov M, Winkler S, Lipinski KA, Tomancak P. A toolkit for high-throughput, cross-species gene engineering in Drosophila. Nat Methods. 2009;6(6):435-7.

51. Sarov M, Schneider S, Pozniakovski A, Roguev A, Ernst S, Zhang Y, et al. A recombineering pipeline for functional genomics applied to Caenorhabditis elegans. Nat Methods. 2006;3(10):839-44.

52. Wu F, Levchenko I, Filutowicz M. Binding of DnaA protein to a replication enhancer counteracts the inhibition of plasmid R6K gamma origin replication mediated by elevated levels of R6K pi protein. J Bacteriol. 1994;176(22):6795-801. PMCID: 197046.

53. Huang CJ, Tu CT, Hsiao CD, Hsieh FJ, Tsai HJ. Germ-line transmission of a myocardium-specific GFP transgene reveals critical regulatory elements in the cardiac myosin light chain 2 promoter of zebrafish. Dev Dyn. 2003;228(1):30-40.

54. Abe K, Hazama M, Katoh H, Yamamura K, Suzuki M. Establishment of an efficient BAC transgenesis protocol and its application to functional characterization of the mouse Brachyury locus. Exp Anim. 2004;53(4):311-20.

55. Foley JE, Maeder ML, Pearlberg J, Joung JK, Peterson RT, Yeh JR. Targeted mutagenesis in zebrafish using customized zinc-finger nucleases. Nat Protoc. 2009;4(12):1855-67. PMCID: 2814337.

56. Doyon Y, McCammon JM, Miller JC, Faraji F, Ngo C, Katibah GE, et al. Heritable targeted gene disruption in zebrafish using designed zinc-finger nucleases. Nat Biotechnol. 2008;26(6):702-8. PMCID: 2674762.

57. Klug A. The discovery of zinc fingers and their development for practical applications in gene regulation and genome manipulation. Q Rev Biophys. 2010;43(1):1-21.

58. Porteus MH, Carroll D. Gene targeting using zinc finger nucleases. Nat Biotechnol. 2005;23(8):967-73.

59. Bitinaite J, Wah DA, Aggarwal AK, Schildkraut I. FokI dimerization is required for DNA cleavage. Proc Natl Acad Sci U S A. 1998;95(18):10570-5. PMCID: 27935.

60. Bibikova M, Golic M, Golic KG, Carroll D. Targeted chromosomal cleavage and mutagenesis in Drosophila using zinc-finger nucleases. Genetics. 2002;161(3):1169-75. PMCID: 1462166.

61. Karlsson J, von Hofsten J, Olsson PE. Generating transparent zebrafish: a refined method to improve detection of gene expression during embryonic development. Mar Biotechnol (NY). 2001;3(6):522-7.

62. Curado S, Stainier DY, Anderson RM. Nitroreductase-mediated cell/tissue ablation in zebrafish: a spatially and temporally controlled ablation method with applications in developmental and regeneration studies. Nat Protoc. 2008;3(6):948-54. PMCID: 2705989.

63. Curado S, Anderson RM, Jungblut B, Mumm J, Schroeter E, Stainier DY. Conditional targeted cell ablation in zebrafish: a new tool for regeneration studies. Dev Dyn. 2007;236(4):1025-35.

64. Court DL, Sawitzke JA, Thomason LC. Genetic engineering using homologous recombination. Annu Rev Genet. 2002;36:361-88.

65. Shizuya H, Birren B, Kim UJ, Mancino V, Slepak T, Tachiiri Y, et al. Cloning and stable maintenance of 300-kilobase-pair fragments of human DNA in Escherichia coli using an F-factor-based vector. Proc Natl Acad Sci U S A. 1992;89(18):8794-7. PMCID: 50007.

66. Heermann R, Zeppenfeld T, Jung K. Simple generation of site-directed point mutations in the Escherichia coli chromosome using Red(R)/ET(R) Recombination. Microb Cell Fact. 2008;7:14. PMCID: 2373285.

67. Kawakami K, Shima A, Kawakami N. Identification of a functional transposase of the Tol2 element, an Ac-like element from the Japanese medaka fish, and its transposition in the zebrafish germ lineage. Proc Natl Acad Sci U S A. 2000;97(21):11403-8. PMCID: 17212.

68. Urasaki A, Morvan G, Kawakami K. Functional dissection of the Tol2 transposable element identified the minimal cis-sequence and a highly repetitive sequence in the subterminal region essential for transposition. Genetics. 2006;174(2):639-49. PMCID: 1602067.

69. Shiraki T, Kojima D, Fukada Y. Light-induced body color change in developing zebrafish. Photochem Photobiol Sci. 2010;9(11):1498-504.

70. Burgess HA, Granato M. Modulation of locomotor activity in larval zebrafish during light adaptation. J Exp Biol. 2007;210(Pt 14):2526-39.

71. Weinstein BM. Big fish in the genome era. Brief Funct Genomic Proteomic. 2008;7(6):411-4. PMCID: 2722260.

72. Meng X, Noyes MB, Zhu LJ, Lawson ND, Wolfe SA. Targeted gene inactivation in zebrafish using engineered zinc-finger nucleases. Nat Biotechnol. 2008;26(6):695-701. PMCID: 2502069.

73. Klug A. The discovery of zinc fingers and their applications in gene regulation and genome manipulation. Annu Rev Biochem. 2010;79:213-31.

74. Reed GH, Wittwer CT. Sensitivity and specificity of single-nucleotide polymorphism scanning by high-resolution melting analysis. Clin Chem. 2004;50(10):1748-54.

75. Philp AR, Garcia-Fernandez JM, Soni BG, Lucas RJ, Bellingham J, Foster RG. Vertebrate ancient (VA) opsin and extraretinal photoreception in the Atlantic salmon (Salmo salar). J Exp Biol. 2000;203(Pt 12):1925-36.

76. Robertson GN, McGee CA, Dumbarton TC, Croll RP, Smith FM. Development of the swimbladder and its innervation in the zebrafish, Danio rerio. J Morphol. 2007;268(11):967-85.

77. Lindsey BW, Smith FM, Croll RP. From inflation to flotation: contribution of the swimbladder to whole-body density and swimming depth during development of the zebrafish (Danio rerio). Zebrafish. 2010;7(1):85-96.

78. Cerveny KL, Cavodeassi F, Turner KJ, de Jong-Curtain TA, Heath JK, Wilson SW. The zebrafish flotte lotte mutant reveals that the local retinal environment promotes the differentiation of proliferating precursors emerging from their stem cell niche. Development. 2010;137(13):2107-15. PMCID: 2882130.

79. Jia S, Nakaya N, Piatigorsky J. Differential expression patterns and developmental roles of duplicated scinderin-like genes in zebrafish. Dev Dyn. 2009;238(10):2633-40. PMCID: 3112361.

80. Jia S, Omelchenko M, Garland D, Vasiliou V, Kanungo J, Spencer M, et al. Duplicated gelsolin family genes in zebrafish: a novel scinderin-like gene (scinla) encodes the major corneal crystallin. Faseb J. 2007;21(12):3318-28.

81. Schartau JM, Sjogreen B, Gagnon YL, Kroger RH. Optical plasticity in the crystalline lenses of the cichlid fish Aequidens pulcher. Curr Biol. 2009;19(2):122-6.

82. Jester JV, Moller-Pedersen T, Huang J, Sax CM, Kays WT, Cavangh HD, et al. The cellular basis of corneal transparency: evidence for 'corneal crystallins'. J Cell Sci. 1999;112 (Pt 5):613-22.

83. Soules KA, Link BA. Morphogenesis of the anterior segment in the zebrafish eye. BMC Dev Biol. 2005;5:12. PMCID: 1183199.

84. Yoshikawa S, Norcom E, Nakamura H, Yee RW, Zhao XC. Transgenic analysis of the anterior eye-specific enhancers of the zebrafish gelsolin-like 1 (gsnl1) gene. Dev Dyn. 2007;236(7):1929-38.

85. Vihtelic TS, Fadool JM, Gao J, Thornton KA, Hyde DR, Wistow G. Expressed sequence tag analysis of zebrafish eye tissues for NEIBank. Mol Vis. 2005;11:1083-100.

86. Easter SS, Jr., Nicola GN. The development of vision in the zebrafish (Danio rerio). Dev Biol. 1996;180(2):646-63.

87. Guido ME, Garbarino-Pico E, Contin MA, Valdez DJ, Nieto PS, Verra DM, et al. Inner retinal circadian clocks and non-visual photoreceptors: novel players in the circadian system. Prog Neurobiol. 2010;92(4):484-504.

88. Jenkins A, Munoz M, Tarttelin EE, Bellingham J, Foster RG, Hankins MW. VA opsin, melanopsin, and an inherent light response within retinal interneurons. Curr Biol. 2003;13(15):1269-78.

89. Hankins MW, Peirson SN, Foster RG. Melanopsin: an exciting photopigment. Trends Neurosci. 2008;31(1):27-36.

90. Foster RG. Photoentrainment of Vertebrate Circadian Rythms. In: Kumar V, editor. Biological Rythms. New Delhi, India: Narose Publishing House; 2002.

91. Halstenberg S, Lindgren KM, Samagh SP, Nadal-Vicens M, Balt S, Fernald RD. Diurnal rhythm of cone opsin expression in the teleost fish Haplochromis burtoni. Vis Neurosci. 2005;22(2):135-41.

92. Foster RG, Bellingham J. Inner retinal photoreceptors (IRPs) in mammals and teleost fish. Photochem Photobiol Sci. 2004;3(6):617-27.

93. MacNeil MA, Masland RH. Extreme diversity among amacrine cells: implications for function. Neuron. 1998;20(5):971-82.

6 Appendices

6.1.Used Software

ApE plasmid editor

http://biologylabs.utah.edu/jorgensen/wayned/ape/

Applied Biosystems HRM (High Resolution Melting Curve) Software v2.0

http://www.appliedbiosystems.com

Augustus gene prediction

http://augustus.gobics.de/

CLC Main Workbench 5.7.1

http://www.clcbio.com/

EnsEMBL genome browser

http://www.ensembl.org/index.html

NCBI webserver

http://www.ncbi.nlm.nih.gov/

NEBcutter v2.0

http://tools.neb.com/NEBcutter2/

Softberry gene prediction

http://linux1.softberry.com/berry.phtml

ZFN target site algorithm

http://pgfe.umassmed.edu/ZFPsearch.html

6.2.BAC IDs and locations retrieved from ENSEMBL genome browser

Gene	BAC ID	Location (according to ENSEMBL)	BAC backbone	Remarks
tmtopsa1	zC41F6.ya	24:26858573:27051242	pTarBAC2.1	contains whole genomic locus of *tmtopsa1* with app. 70 kb of 5' upstream sequence
tmtopsb1	zC226G17.za	9:6117362:6312818	pTarBAC2.1	comprises whole genomic locus of *tmtopsb1* with app. 64 kb of 5' upstream sequence
tmtopsb2	zC161K7.za	6:16529555:16681751	pTarBAC2.1	contains exon 1 and 2 of *tmtopsb2* with app. 99 kb of 5' upstream sequence
enc	zC246H18.za	13:42890423:43052569	pTarBAC2.1	contains whole genomic locus of *enc* with only app. 20 kb of 5' upstream sequence

6.3.Technical protocol for BAC recombineering

A recombination cassette flanked by 50bp homology arms was amplified in a PCR using the Finnzymes Phusion polymerase in five 50µl HFBuffer reactions according to the manufacturer's manual. The following PCR program was used for this: 94°C for 5 minutes, followed by 35 cycles with 94°C for 10 minutes, 62°C for 1 minute and 72°C for 1 minute, another 72°C for 5 minutes and storage at 10°C. The PCR reactions were pooled and gel-eluted using a 1% SYBRsave gel and the Qiagen DNA extraction kit. Unless the cassette was amplified from a plasmid containing the R6K origin of replication, a DpnI digest was performed to avoid unwanted vector contaminations. For this 1µl DpnI (NEB) and 5µl NEBuffer 4 were added to 44 µl eluat and the mixture was incubated at 37°C for 30 minutes. The enzyme was then removed using the Qiagen PCR Purification Kit and the cassette was eluted in 50µl ddH_2O. The amount of PCR product was estimated on a 1% agarose gel and 4-8 µl of the cassette were used for transformation of electro-competent DH10B E. coli carrying the respective BAC.

For this bacteria were grown over night in LB-chloramphenicol in a 1ml liquid culture. 20 µl of this culture were used to inocculate 1,4ml fresh LB-chloramphenicol and grown at 37°C for approximately 2 hours until an OD_{600} of 0,3. The OD_{600} was measured on the Nanodrop.

First bacteria were transformed with approximately 10ng of the plasmid pRed/ET or pRedFlp4 respectively. For the transformation with the recombination cassette an induction with 10% L-arabinose or 25% L-rhamnose respectively by shaking at 37°C for 60 minutes is necessary. Before electroporation the bacteria were washed three times with pre-chilled 10% glycerol by spinning down the cells for 30 seconds at 11000 rpm and 4°C, removing the supernatant and resupending the cells in glycerol. After the last wash residual supernatant was taken off with the pipet and the bacteria were kept on ice. After adding the plasmid or recombination cassette to the tube the cells were electroporated using the following settings: 2,5 kV, 25µF, 200 Ω.

After this 1 ml of LB without antibiotics was immediately added to the bacteria and the cells were incubated for 70 minutes at 30°C in the case of transformation with the Red/ET plasmid and at 37°C in the case of transformation with a homology cassette.

The bacteria were then plated on LB-plates containing the appropriate antibiotics using glass beads and incubated for a minimum of 20 hours at 30°C or over night at 37°C if the Red/ET expression plasmid was no longer needed for further recombination.
For a more detailed recombination protocol see the manual of the Counter-Selection BAC Modification Kit (Gene Brigdes, www.genebridges.com)

6.4.Microinjection of Zebrafish and Medaka

For injections into Zebrafish zygotes couples were set up as described above. The eggs were collected in a petridish containing 1xE3. Fertilized eggs were transfered into an injection dish containing solidified 1,5% agarose in 1xE3 creating triangular furrows into which the embryos can be sorted using forceps. Medaka embryos were scraped of the females bellys as described before and collected in chilled 1xERM to slow down embryonal development. For Medaka injections the same injections dishes were prepared with 1,5% agarose in 1xERM. Here the embryos were fixed in rectangular furrows of the agarose layer using forceps.
For the injections the injections dishes were placed under a Zeiss Binocular and the embryos were arranged in a way that the fertilized cell faces upwards toward the injection needle. Needles for injection into Zebrafish (Science Products, GB100F-10 (0:58x1x100mm) Medaka and GB100TF10 (0:78x1x100mm) differ in their diameter and thickness. For Zebrafish a very fine needle with a longer tip is used, for Medaka a thicker tip is necessary to penetrate the thick chorion. Needles were pulled using the Sutter Instrument Flaming/Brown Micropipette Puller. For Medaka needles the following settings were used: pressure 500, heat 580, pull 30, velocity 35, time 150. For Zebrafish needles the program was pressure: 500, heat: 510, pull: 100, velocity: 170, time: 120.
The needle was fixed in a needle holder that is connected to the InjectMan NI2 and the FemtoJet -express- which regulates the pressure with which the solution is injected.
Injected embryos were screened for the presences of the injection marker TRITC under the StereoLumar and raised to adulthood in the case of Zebrafish or frozen in liquid nitrogen at 2dpf in the case of Medaka.

6.5.Zinc Finger Sites for targeted gene knock-out in Medaka

For targeted gene knock-out of Medaka *tmtopsb* and *tmtopsa1* the following Zinc Finger Nuclease recognition sites were chosen using a zinc finger target site algorithm (Scot Wolfe, http://pgfe.umassmed.edu/ZFPsearch.html).

For amplification of the respective ZFPs the following primers were used:

ZFP1: ZFN_F1_Acc65I_fw GCGATGGGTACCCGCCCATATGCTTGC/
ZFN_F1_rev CACTGGAAGGGCTTCTGGCCTGTGTGAATCCGGATGTG

ZFP2:ZFN_F2_fw CATCCGGATTCACACAGGCCAGAAGCCCTTCCAGTGTCGCATCTGC/
ZFN_F2_rev ATGTCGCATGCAAAAGGCTTCTCGCCTGTGTGGGTGCGGATGTG

ZFP3: ZFN_F3_fw CGAGAAGCCTTTTGCATGCGACA/
ZFN_F3_BamHI_rev GCGTAGGATCCACCTGTGTGGATCTTGGTGTG

After generating the individual ZFPs a PCR with a mix of the three Finger fragments and the primers ZFN_F1_Acc651_fw and ZFN_F3_BamHI was performed to amplifiy the whole three-finger ZFP. The sequences of the ZFN target sites and respective 3’ and 5’ fingers are summarized in the following table, as well as the respective templates for the individual ZFPs.

Gene	Exon	position	ZFN site	5pZF	3pZF	5p vectors (stock#)	3p vectors (stock#)
tmtopsa1	2	418	aCGCCCAACAtggccGACGGCAGGg	TGT-TGG-GCG	GAC-GGC-AGG	Z-F4/Z-D9/Z-B1	Z-E4/Z-D3/Z-A3
tmtopsa1	2	399	gCGCTACTCCaccgtGATGACGCCc	GGA-GTA-GCG	GAT-GAC-GCC	Z-E8/Z-D5/Z-B1	Z-E5/Z-A5/Z-A12
tmtopsb	1	276	cTTCGCCTCCagcatcCGGGGGAGGt	GGA-GGC-GAA	CGG-GGG-AGG	Z-E8/Z-D3/Z-A7	Z-E3/Z-F6/Z-A3
tmtopsb	1	282	cTCCAGCATCcggggGAGGTGGCTg	GAT-GCT-GGA	GAG-GTG-GCT	Z-E5/Z-D1/Z-B3	Z-D4/Z-B3/Z-B2

Zinc Finger target sites of *O.l. tmtopsa1 and tmtopsb*

The Zinc Finger target sites and respective ZFPs are summarized here. Note that for both the 5' ZFP and the 3' ZFP the individual ZF-tripletts are listed in the order ZF3-ZF2-ZF1.

ZFN PLATE VECTORS					
ZF1		**ZF2**		**ZF3**	
Z-A3	pBS-F1-AAG	Z-A5	1352-F1-CAG-F2-GAC	Z-D4	pBS-F3-GAG
Z-A7	pBS-F1-GAA	Z-B3	1352-F1-GGA-**F2-GTG**-F3-T	Z-E3	pBS-F3-CGG
Z-A1	pBS-F1-GCC	Z-D1	pBS-F2-GCT	Z-E4	pBS-F3-GAC
Z-B1	1352-F1-GCG	Z-D3	1352-F2-GGC	Z-E5	1352-F3-GAT
Z-B2	1352-F1-GCT	Z-D5	pBS-F2-GTA	Z-E8	pBS-F3-GGA
Z-B3	1352-**F1-GGA**-F2-GTG-F3-T	Z-D9	1352-F2-TGG	Z-F4	1352-F3-TGT
		Z-F6	1352-F2-GGG		

Plasmids and stock numbers for modular assembly of three finger ZFPs from ZFN Plate

6.6.Primer Sequences

The following table contains the sequences of all primers that were used in the course of the project.

STOCK #	OLIGO NAME	ORGANISM/VECTOR	SEQUENCE	LENGTH	PURPOSE
979	**A1_for1**	*Danio rerio*	CTCCAGAACCACAGAAACGATGGG	24	**BAC recombineering, colony PCR for BAC verification and identification of recombined clones**
980	**A1_for2**		TTAGAAAACTCTCCAAAACTTAAATGGA	28	
981	**A1_rev1**		ACATTGTAGCGATTGAAGCATCT	23	
982	**A1_rev2**		AATCAGACATGTGCATTCAAACCC	24	
983	**B1_for1**		CAGTTAAATTCGTGCTTCTTACTTCGAGA	29	
984	**B1_for2**		AATCCAGCAGACTCGAACGAACT	23	
985	**B1_rev1**		CCATATTTGTGTTTGAGTTTTGGAGATGTAG	31	
986	**B1_rev2**		ACTACCGCTCACAGCGTGTAAAAACC	26	
1055	**B1_ATG_for1**		ATGAGCGAGGAAGACCGCTTAAC	23	
1056	**B1_ATG_for2**		CTTCTGGACGAGGACTGGAGCGA	23	
1057	**B1_TAG_rev1**		GAAGCAGGAGTTGATGAAGCCG	22	
1058	**B1_TAG_rev2**		TACCACATGCAGCCGTGTCGC	21	
1262	**DrB2 for 1**		AGCATGGTCCACTCTCGGTTGTG	23	
1263	**DrB2 for 2**		GAGTAGCTCCGATAGAATTTTATCC	25	
1264	**DrB2 rev 1**		GGCTACCTCAGCATTTAAGCTGT	23	
1265	**DrB2 rev 2**		GTTAAACAGATTCAAATTTAGTTCC	25	
975	**Enc_for1**		CTGCTCTACTACCCTGAATCCC	22	
976	**Enc_for2**		TCTGCTGAATCGGGTCACTCAC	22	
977	**Enc_rev1**		CCAAGTAGCCTTCAAACGCGTAAA	24	
978	**Enc_rev2**		TATATGCGCATTTCTTTCTTAATTTGTCTCATAAAG	36	
1059	**A1_rpsLneo_for**		ACAAAACCAAACTCATTAAATCCTTTACACAAGCCATAATTAATGGTGCAGGCCTGGTGATGATGGCGGGATCG	74	**Primers for amplification of homology cassette for BAC recombineering; Primer adds 50 bp homology arms for the respective opsin to the *rpsLneo* or *egfp/e2n* fragment**
1060	**A1_rpsLneo_rev**		CCCTATTTTAATTGTTTTAATGACATCGCTGTAACATACAGCAGACTCACTCAGAAGAACTCGTCAAGAAGGCG	74	
1067	**DrA1_E2N for**		ACAAAACCAAACTCATTAAATCCTTTACACAAGCCATAATTAATGGTGCAATGGTGAGCAAGGGCGAGGA	70	
1068	**DrA1_E2N rev**		CCCTATTTTAATTGTTTTAATGACATCGCTGTAACATACAGCAGACTCACAAAAAACCTCCCACACCTCCCC	73	
1260	**DrB1_E2N for**		GAACTTTTTTAGCTATGTTTTTCGAGCAGGCCGATTTAAACTACAGCTTCAACATGGTGAGCAAGGGCGAGGA	73	
1261	**DrB1_FRT rev**		AAACCCATTAAACTTTCTAAAAGCATTTGGTTATTGACGTCTGATTACGTACCGGTCTTTATAATCCTCGAGC	73	
1336	**DrB2_E2N for**		GGATCAAGGACGCAGTAAACGTAACATCAGTTGAAAACTGTGCGGCAAAGATGGTGAGCAAGGGCGAGGAGCTGT	76	
1337	**DrB2_FRT_rev**		CGCCGTATGCATATTTTGTTTGTTTGTTTGTTTGTTTGTTTTGTTGTTTGTGTTTACTCACCTAGGTCTTTATAATCCTCGAGC	88	
1061	**Enc_rpsLneo_for**		CTTCGGATGCTATTGAGAGTCACCATGTTGGGAGTTGACTTGGAAAAGAAGGCCTGGTGATGATGGCGGGATCG	74	
1062	**Enc_rpsLneo_rev**		TTAAAACTTCCTCATGTGACTCTAGATAAATAAATAGAGACATAACTGACTCAGAAGAACTCGTCAAGAAGGCG	74	
1069	**DrEnc_E2N for**		CTTCGGATGCTATTGAGAGTCACCATGTTGGGAGTTGACTTGGAAAAGAAATGGTGAGCAAGGGCGAGGA	70	
1070	**DrEnc_E2N rev**		TTAAAACTTCCTCATGTGACTCTAGATAAATAAATAGAGACATAACTGACAAAAAACCTCCCACACCTCCCC	72	
1161	**EGFP for1**	EGFP_N1 (Clonetech)/ rpsLneo (Genebridges)	CGAATTCTGCAGTCGACGGTACCGCGGGCCCG	32	**Cloning of *egfp_rpsLneo* fusion cassette for BAC Recombineering**
1162	**EGFP for 2**		GGATCCACCGGTCGCCACCATGGTGAGCAAGGG	33	
1160	**EGFP_rpsLneo rev**		GATCCCGCCATCATCACCAGGCCACGCCTTAAGATACATTGATGAGTTTGGACAAACCACAACTAGAATGC	59	
1155	**EGFPrpsLneo_ctfusion for**		CCAAACTCATCAATGTATCTTAAGGCGTGGCCTGGTGATGATGGCGGGA	49	
1159	**rpsLneo_rev**		TCAGAAGAACTCGTCAAGAAGGCG	25	
1332	**DrA1_BH_tol2_clmc2 for**	*Danio rerio*	GTTGAATAGAGCGTTTGGACCCGGAAGCCGCTCCGCGTGACGTCACACTTCAAGTACTTTACACCTCTGGGATCTTCACCTAGATCCTT	90	**Amplicication of cmlc2:mcherry (bleeding heart) cassette for integration into zC41F6.ya (*tmtopsa1*) genomic sequence**
1333	**DrA1_BH_tol2_clmc2 rev**		ACAAGTGACTAGTAATGTTGGAAATCTACTAGCCACAGTGGCTGGTGATCGGATCATAATCAGCCATACCAC	72	
1420	**A1_seq_R**		GTGGACATAACACAGCATCTAAATC	26	**Primers for BAC sequencing**
1421	**SV40_seq_R**	EGFP-N1	CTCATCAATGTATCTTATCATGTCTGG	27	
1255	**SV40_F**		GATCCAGACATGATAAGATAC	22	
1256	**EGFP_R**		CGCCGTCCAGCTCGACCAGGA	22	
1422	**cmlc2_seq_F**	*cmlc2:mcherry*	GCCAGTGACCCAGGAGCCCAGACC	24	
64	**ZFN_F1_Acc65I_fw**	Worcester ZFN library	GCGATGGGTACCCGCCCATATGCTTGC	27	**Amplification of individual Zinc Finger Proteins**
65	**ZFN_F1_rev**		CACTGGAAGGGCTTCTGGCCTGTGTGAATCCGGATGTG	38	
66	**ZFN-F2_fw**		CATCCGGATTCACACAGGCCAGAAGCCCTTCCAGTGTCGCATCTGC	46	
67	**ZFN_F2_rev**		ATGTCGCATGCAAAAGGCTTCTCGCCTGTGTGGGTGCGGATGTG	44	
68	**ZFN_F3_fw**		CGAGAAGCCTTTTGCATGCGACA	23	
69	**ZFN_F3_BamHI_rev**		GCGTAGGATCCACCTGTGTGGATCTTGGTGTG	32	
1026	**ZFN_B1for_XhoI**	*Oryzias latipes*	TACTCGAGCATGACCTTCGGCTTCCTCAACA	31	**Amplification of Zinc Finger Target site from genomic DNA for ZFN read-out**
1142	**B1_ZFN rev_EcoRI**		TAGAATTCCCAAAGCAGGAGTTGATGAAG	29	
1085	**ZFN DD for**	Worcester ZFN library	CAGCCAGAAGGGGCACCTCACCCC	24	**Colony PCR for Zinc Fingers subcloned into the respective FokI expression vector**
1086	**ZFN DD rev**		TGTGCTTCCTGAGCGCGTCGCTG	23	
1087	**ZFN RR for**		CCGTAGCGACGCGCTCACCC	20	
1088	**ZFN RR rev**		TATGGCGGGTGAGGTTAGACAACTG	25	
1353	**OlB1_F**	*Oryzias latipes*	CAGCGTCAGCGACATGCTGGT	21	**Cloning of a control construct for HRM test run**
1354	**OlB1_Fusion F**		GCTCAGCTTCGCCTCCAGCATATCCCTGGACCTGCAGCTTAGG	43	
1355	**OlB1_Fusion F**		CCTAAGCTGCAGGTCCAGGGATACAGCAGCCACCTCCCCCGGA	43	
1503	**pTarBac_cmlc2_fw**	pTarBAC2.1	GCGTAAGCGGGGCACATTTCATTACCTCTTTCTCCGCACCCGACATAGATCCCTGCTCGAGCCGGGCCCAAGTG	74	**Amplification of piTol2 homology cassette from integration of *cmlc2:mcherry* into BAC backbone pTarBAC2.1**
1504	**pTarBac_cmlc2_R_1**		CGCGGGGCATGACTATTGGCGCGCCGGATCGATCCTTAATTAAGTCTACTACAGGAAACAGCTATGACCATG	72	
1501	**pTarBac F**		GGCAGTTATTGGTGCCCTTAAACGCC	27	**Colony PCR**
1502	**pTarBac R**		CTGGGTTTAAACCCGGATCATGCATC	27	

7 Abstract

Most organisms on the planet depend on light as a source of information to synchronize biological events. In order to regulate physiological and behavioural processes, animals employ non-image forming photoreceptors to perceive photic information. In vertebtrates non-visual photoreception has been believed to be restricted to the retinal ganglion cells of the eye and the pineal gland, however evidence exists that additional photoreceptive sites are present deep inside the brain throughout the anterior nervous system. On a molecular basis Opsins are the candidate molecules to mediate non-image forming light detection. In the course of my project I focus on two novel families of highly conserved non-visual Opsins, namely the Teleost Multiple Tissue Opsins and Encephalopsin.The two teleost species *Danio rerio* and *Oryzias latipes* both possess a wide spectrum of these novel classes of photopigments, whose function is still unclear. By employing whole mount *in situ* hybridisation, transgenesis and zinc- finger mediated mutagenesis I approach the characterization of these deep brain photoreceptors in Zebrafish and Medaka to investigate their biological role. Expression analysis showed that there is a relatively high abundance of photoreceptive sites within the vertebrate brain. This suggests, that the brain does not only receive and integrate information from the periphery, but is indeed directly involved in the sensory process.

8 Zusammenfassung

Für die meisten Organismen auf diesem Planeten dient das Licht als Informationsquelle für die Synchronisation bestimmter biologischer Prozesse. In Tieren wird diese Information von Photorezeptoren, welche nicht in den bildgebenden visuellen Prozess eingebunden sind, aufgenommen und über diesen Weg werden physiologische und verhaltenbiologische Phänomene gesteuert. Bisher wurde angenommen, dass in Vertebraten die nicht-visuelle Photorezeption vornehmlich in den retinalen Ganglionzellen der Augen und in der Zirbeldrüse (*glandula pinealis*) stattfindet, allerdings befinden sich nachweislich zusätzliche photorezeptive Areale innerhalb des Gehirns und gesamten anterioren Nervensystems. Auf molekularer Ebene ermöglichen Opsine die nicht-visuelle Lichtwahrnehmung. Im Zuge meines Projektes beschäftige ich mich mit zwei erst relativ kürzlich entdeckten, hoch konservierten Familien der " non-visual Opsins", den Teleost Multiple Tissue Opsinen und Encephalopsin. In den beiden Teleost Arten *Danio rerio* und *Oryzias latipes* finden sich relativ viele Mitglieder dieser Klasse von Photopigmenten, deren Aufgabe jedoch unbekannt ist. Ich bearbeitete die Frage der Funktion dieser „deep brain" Photorezeptoren, indem ich sie in Whole Mount *in situ* Analysen, über Zinc-Finger Mutagenese und Transgenese in Zebrafish und Medaka weiter charakterisierte.

Expressionsanalysen zeigten dass sich im Gehirn von Vertebraten weitreichende photosensorische Areale befinden, was vermuten lässt, dass das Gehirn nicht nur Informationen aus der Peripherie erhält und prozessiert, sondern dass es direkt in den sensorischen Prozess eingebunden ist.

9 Curriculum Vitae

Susanne Bloch

Born:	21.01.1985 in Passau, Germany
Citizenship:	German
Address:	Pfeilgasse 7/10, A-1080 Vienna
Phone:	+43 650 3503848
E-mail:	susannebloch@yahoo.de

EDUCATION

Since October 2005	**University of Vienna (A)** Studies of Molecular Biology
May 2010 – May 2011	**University of Vienna,** Max F. Perutz Laboratories, Group Tessmar-Raible,Diploma Thesis: *Towards the Functional characterisation of Inner Brain Opsins in Medaka and Zebrafish*
October 2004 – July 2005	**Philips-Universität** Marburg (G) Studies of Medicine
June 2004	Graduation from the **Gymnasium Leopoldinum** Passau (G)
1995 – 2004	**Gymnasium Leopoldinum** Passau (G) high school

WORK EXPERIENCE AND EXTRACURRICULAR ACTIVITIES

May 2011	**University of Vienna** Max F. Perutz Laboratories, Group Tessmar-Raible 2-week tutorial: *Laboratory course in developmental biology and molecular neurobiology*
Februar 2010- März 2010	**University of Vienna** Max F. Perutz Laboratories, Group Warren, 2-month rotation: *Depletion of Centrin2 in Trypanosoma brucei utilizing the FKBP-Shield1 System*

Dezember 2009- Januar 2010	**University of Vienna** Max F. Perutz Laboratories, Group Kragler, 5-week rotation: *Identification of MPB2C binding partners in Arabidopsis thaliana*
February 2009	**University of Vienna** Max F. Perutz Laboratories, Group Waldsich, 4-week rotation: *Do DEAD box proteins assist td group I intron splicing in vitro?*
March - April 2008	**Uppsala University**, Uppsala (SE) Dept Photochemistry and Molecular Science, Group Lindblad, Six-week rotation: *The minCDE gene Region in Nostoc punctiforme*
February – April 2005	**Klinikum Passau**, Passau (G) Internship at a hospital

LANGUAGES

German	mother tongue
English	fluent (oral and written)
Italian	good knowledge
Swedish	basic knowledge: Swedish Course at the University of Vienna